ARCHIVES OF ACOUSTICS
9, 4, 273-289 (1984)

A METHOD FOR OBJECTIVE EVALUATION OF THE SENSATION OF THE LOCALISATION DIRECTION OF A SOUND SOURCE

RYSZARD MAKOWSKI

Institute of Telecommunication and Acoustics, Wrocław Technical University
(50-317 Wrocław, ul. B. Prusa 53/55)

This paper proposes a new method allowing the evaluation of the sensation of the localisation direction of an image sound source, generated by signals transmitted by a two - channel loudspeaker stereo - system. This evaluation can be carried out on the basis of the localisation parameters of signals reaching the membrane of the listener's ear drum, i.e. it does not require psychoacoustic investigations. The method proposed takes into account the properties of the human hearing organ, as known from psychoacoustic investigations, which are essential in localisation.

In the final part of the paper, by using the method proposed, a critical evaluation is carried out of a two - channel loudspeaker intensity stereo - system.

1. Introduction

The sensation of sound spatiality, generated by signals reaching the listener's ears directly or through a stereophonic system, is shaped by a large number of factors [3, 4, 9-11, 18]. The evaluation of their effect on the sensation of spatiality is commonly carried out by using psychoacoustic investigations. However, as the number of these factors is large and the psychoacoustic investigations are very time - consuming, the results obtained do not permit comprehensive and thorough analysis of the phenomenon, particularly in the case of stereophonic systems.

The sensation of sound spatiality is also evaluated, in addition to psychoacoustic investigations, by means of other research methods. These methods can be divided into two principal groups. The basic element of one of them is constituted by measurements of changes in the parameters of signals on the path between the sound source and the listener's ears, performed by using an acoustic head analogue or a listener [1, 5, 8, 16]. The other is based on analysis

of phenomena occurring during the transmission of the signals, by using mathematical models [2, 9, 11, 12]. These objective methods permit the determination of the parameters of signals reaching the listener's ears, but give no answer as to what sensation of spatiality is caused by these signals. Thus, there is the need for developing a method which would provide an answer to this question. This need has been pointed out e.g. by BLAUERT [3].

Spatial hearing is a property of the human hearing organ which consists of a large number of elements. FURDUEV [4] distinguishes three components of spatial hearing:

– localisation of sound sources,
– distinguishing signals,
– acoustic atmosphere.

This paper presents a method permitting objective evaluation of the basic component of spatial hearing which is the localisation of sound sources. In developing the method, both the results of psychoacoustic investigations and those of objective measurements of the responses of the external auditory system of man were used. The development of this method required:

– the definition of the so - called localisation parameters, i.e. those parameters of signals reaching the membrane of the listener's ear drum on the basis of which he localises the sound source (section 2),

– the development of a criterion linking the localisation parameters with the sensation of the localisation direction of a sound source which the listener has (sections 3-7).

The method proposed requires knowledge of the localisation parameters of signals reaching the membranes of the listener's ear drums. For given conditions and a given signal emitted by a sound source these parameters can be determined from measurements or calculated from mathematical models, which describe the passage of the signal from the sound source to the listener's ears.

In the final part of this paper, as an illustration of the possibility of application of the method proposed, the results of evaluation of a two - channel loudspeaker intensity stereo - system are given.

2. Definitions of the localisation parameters

As a result of psychoacoustic investigations, it has been established [6 7, 9, 15, 17] that the listener evaluates the localisation direction of a sound source above all on the basis of the following parameters of signals reaching his ears:

–uniaural sound pressure levels,
– interaural difference between sound pressure levels,
– interaural time delay.

The following parameters of the signals, called localisation parameters below, can be subordinated to the above parameters:

– short - term power spectrum levels L_{SL} and L_{SP} of signals reaching the left and right ears:

$$L_{SL}(f, t_0) = 10 \log \frac{S_L(f, t_0)}{S_0}, \quad L_{SP}(f, t_0) = 10 \log \frac{S_P(f, t_0)}{S_0}, \tag{1}$$

where $S_L(f, t_0)$ and $S_P(f, t_0)$ are the short - term power spectra of the signals for the left and right ears, S_0 is the reference quantity,

– interaural difference between the short - term power spectrum levels, ΔL_S, of signals for the left and right ears:

$$\Delta L_S(f, t_0) = L_{SL}(f, t_0) - L_{SP}(f, t_0), \tag{2}$$

– interaural time delay C_S:

$$C_S(f, t_0) = \tau^*_{SL}(f, t_0) - \tau^*_{SP}(f, t_0), \tag{3}$$

where τ^*_{SL} and τ^*_{SP} are the time delays of a direct wave, describing the passage of a signal from the sound source to the membranes of the ear drums of the left and right ears.

The short - term power spectra occurring in formulae (1) are defined in the following way:

$$S(f, t_0) = \int_{-\infty}^{\infty} W_w(|\tau|) \cos 2\pi f\tau \left[\int_{-\infty}^{t_0} R(t, t-|\tau|)\, W_k(t_0 - t)\, dt \right] d\tau, \tag{4}$$

where $R(t, t-|\tau|)$ is the autocorrelation function of a nonstationary random process, $W_k(t)$ is the window function in the time domain, $W_w(\tau)$ is the window function in the domain of time shift, and t_0 is the moment of the determination of the short - term power spectrum.

In definition (4), the window function $W_k(t)$ permits a property of the human hearing organ, called a time constant, to be taken into account. Among research workers there is difference of opinion as to the shape and length of the window function $W_k(t)$ which describes properly the inertial nature of the hearing organ. In the calculations presented in a further part of this paper, a window function proposed by PENNER [14], described by the following relation, was used:

$$W_k(t) = 1(t)\, 1(T_{S0} - t) \frac{2t}{T_{S0}} \exp\left(-\frac{2t}{T_{S0}} + 1 \right), \tag{5}$$

where $1(t)$ is the Heaviside distribution, T_{S0} is the length of the time constant of hearing; it was assumed that $T_{S0} = 50$ ms.

From the psychoacoustic investigations reported on in MISZCZAK's paper [13], it follows that the listener localises a sound source on the basis of the

initial part of a signal reaching his ears, which results from the resumption of sound emission by the source. This property of hearing is known in the literature as "CREMER's law". The initial part of the signal, as a result of the delay of reflected waves with respect to the direct wave, contains mostly the latter wave. Due to this property of hearing, man can correctly localise sound sources in an interior, despite the fact that the energy of reflected wave is often higher than that of the direct wave. CREMER's law imposes the necessity for evaluating the parameters of signals reaching the listener's ears at the time moments $t_0 = t_c + T_{S0}$, where t_c is the moment when the wave front reaches the listener.

3. Localisation of sound sources in standard conditions

The standard conditions are understood here to be the conditions of direct detection in an open space of a signal emitted by a sound source. In such conditions the signals reaching the listener's ears are determined by the transfer functions of the external auditory system, corresponding to a given localisation of the sound source with respect to the listener, and by the signal emitted by this source [10, 11]. In turn the localisation parameters ΔL_S^B and C_S^B (the index B denotes the standard conditions) depend above all on the transfer functions of the external auditory system and on the localisation direction of the sound source with respect to the listener. In localisation, the parameters L_{SL}^B and L_{SP}^B play an auxiliary function [18] and therefore they will for the time being be neglected. The way of describing the localisation of the sound source with respect to the listener is shown in Fig. 1.

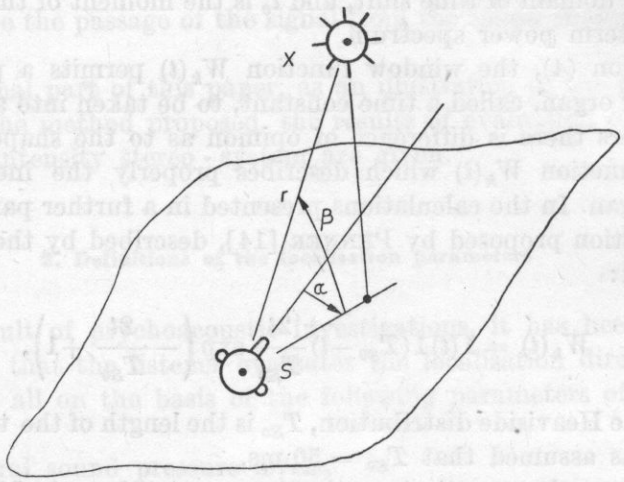

Fig. 1. The localisation of the sound source X with respect to the listener S

The listener can quite easily determine the localisation direction of a real sound source in anechoic conditions. In such conditions localisation is natural. When in the standard conditions the source, situated at an angle (α, β) with respect to the listener, emits a signal with its spectrum concentrated round some frequency f_1, this signal causes a definite time delay $C_S(f_1) = C_S^B(f_1)$ and the difference between short - term spectrum levels, $\Delta L_S(f_1) = \Delta L_S^B(f_1)$. In the standard conditions there is then a function which subordinates the values of ΔL_S^B and C_S^B to given values of f, α, β. Since this subordination is described by a relationship of five quantities, this situation can be represented in a five-dimensional space (ΔL_S, C_S, f, α, β). For definite f, α, β a point is described by a relationship of five quantities. Assumption by f, α and β of all the values within their variability ranges causes a set H^* to be generated. In the space (ΔL_S, C_S, f, α, β) this set will be represented by a line. Points lying on this line will describe all the interrelationships of the five quantities defining the localisation in the standard conditions which are possible for a given listener. Thus, the set H^* constitutes a description of the localisation for direct detection in anechoic conditions.

As a result of visual and auditory experiences, in the process of learning, the listener memorises the interrelationship of the five quantities describing the localisation in the standard conditions. When the system sound source - listener is in anechoic conditions and the listener cannot see the sound source, then, on the basis of the frequency f, the delay C_S^B and the level difference ΔL_S^B, the listener can determine the localisation direction of the sound source, i.e. the angles α and β. This evaluation is possible due to knowledge of the interrelationship of the quantities ΔL_S^B, C_S^B, f, α and β, described by the set H^*. It can thus be stated that the set H^* is a description of a decision - making model of the localisation of sound sources.

In view of the individual feature of their bodily constitutions, for each of listeners there occurs a different interrelationship of the quantities ΔL_S^B, C_S^B, f, α and β. For a given listener this interrelationship is invariable, and so are the shapes of the external auditory system. In the process of learning every one adopts a different subordination, i.e. creates his own set H^*. These individual subordinations constitute individual decision - making models.

4. Averaged decision-making model

In evaluating stereophonic systems it is warranted to use the decision - making model of "the standard listener" who represents the properties of the hearing organs of a human group. Thus, it is necessary to develop an averaged decision - making model. To date, no investigations of the properties of the hearing organ have been carried out with the view to developing an averaged decision - making model, nevertheless measurements have been taken of the "shadow"

effect of the head solid. The results of these measurements were gathered by Shaw and represented in the form of a set of the averaged moduli of the transfer functions from the free field to the membranes of the listener's ear drums, as a function of frequency and the angle α [17]. On the basis of these moduli, using Hilbert's transform, a set of impulse responses of the external auditory system was calculated [10, 11]. In turn these impulse responses became the basic elements of the mathematical model of signal passage from the sound source to the listener's ears in standard conditions. With this model, assuming that the autocorrelation function of a signal emitted by the sound

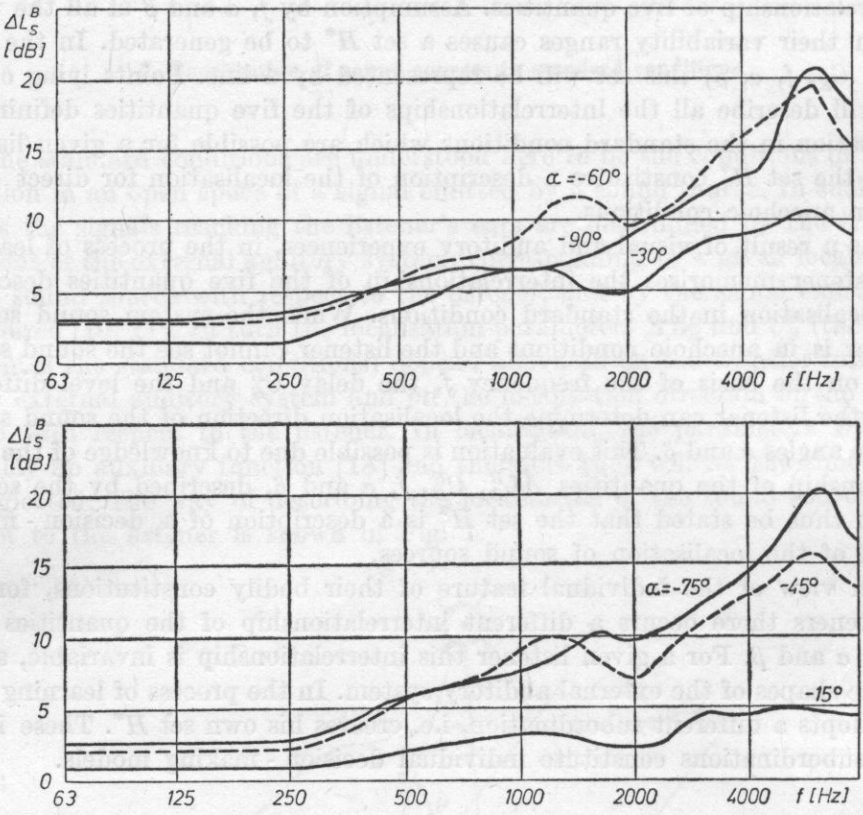

Fig. 2. The differences in the short - term spectral power levels, ΔL_S^B, in standard conditions, for various angles α

source has the form $R_{xx}(t_1, t_2) = {}^2\delta(t_1, t_2)$, where ${}^2\delta(t_1, t_2)$ is a twodimensional Dirac distribution, the dependencies of the level difference ΔL_S^B and the time delay C_S^B on frequency and the horizontal angle α was determined. These dependencies are shown in Figs. 2 and 3.

In view of lack of sufficient data, attempts to determine the effect of the vertical angle β on ΔL_S^B and C_S^B failed. Therefore, considerations were restricted

to the horizontal plane, i.e. to the case $\beta = 0$. This restriction reduces the decision - making model to four dimensions: ΔL_S, C_S, f and α. In practice this has no essential significance, since the localisation of image sound sources in two - channel loudspeaker stereophony should be limited to the horizontal plane. The elevation of an image source, which is observed at times, will from

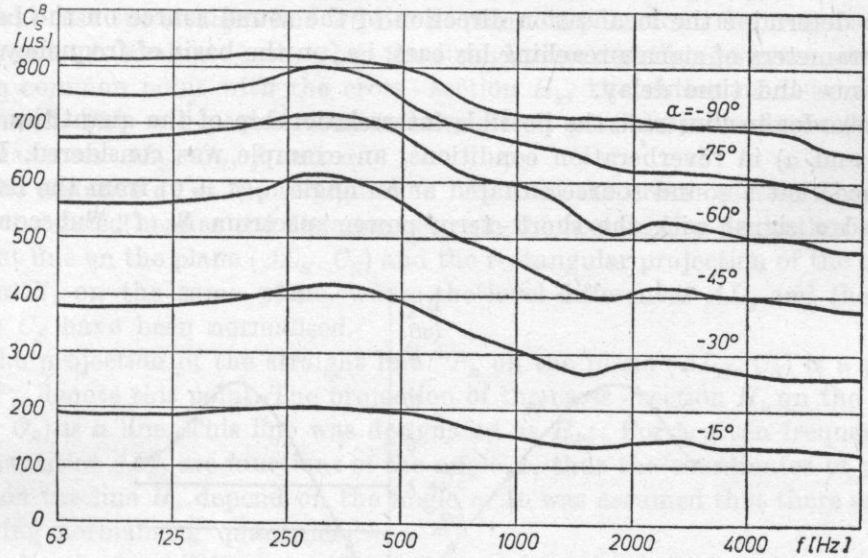

Fig. 3. The time delays C_S^B in standard conditions, for various angles α

this point of view be regarded as disagreement between the effect achieved and the desired one.

The set defined in the fourdimensional space (ΔL_S, C_S, f, α) was designated as H. In this space the set H is represented by a line.

5. Definition of the distance d_k and the angle α_k

The set H describes the interrelationship of the parameters ΔL_S, C_S, the frequency f and the angle α for direct detection in anechoic conditions. In these conditions localisation is obvious and natural. Most frequently, however, the listener will determine the localisation of the sound source in an interior where reflections from the walls occur. These reflections cause a change in the level difference ΔL_S (with respect to anechoic conditions) [10]. There is in turn no change in the time delay C_S, since it is determined by the direct wave. The interrelationship of ΔL_S, C_S, f and α is different from that in standard conditions, and in addition it varies with changing acoustic conditions. When reflections from the walls essentially change the level difference ΔL_S and the listener cannot see the sound source, he can find it difficult to define the locali-

sation direction of the sound source and his localisation can be erroneous [13]. In a case when reflections from the walls do not exert any large effect on ΔL_S, it is not difficult for the listener to determine the localisation direction of the sound source and his localisation is correct. Similar problems can occur for the detection of a signal transmitted by a stereophonic system. In this case, the listener cannot see the sound source. There is an image source. The listener has to determine the localisation direction of the sound source on the basis of the parameters of signals reaching his ears, i.e. on the basis of frequency, level difference and time delay.

In order to illustrate the possible interrelationship of the quantities (ΔL_S, C_S, f and α) in reverberation conditions, an example was considered. It was assumed that a sound source situated at an angle $\alpha_i (\beta = 0)$ from the listener, emitted a signal with the short - term power spectrum $S_{xi}(f)$. Subsequently,

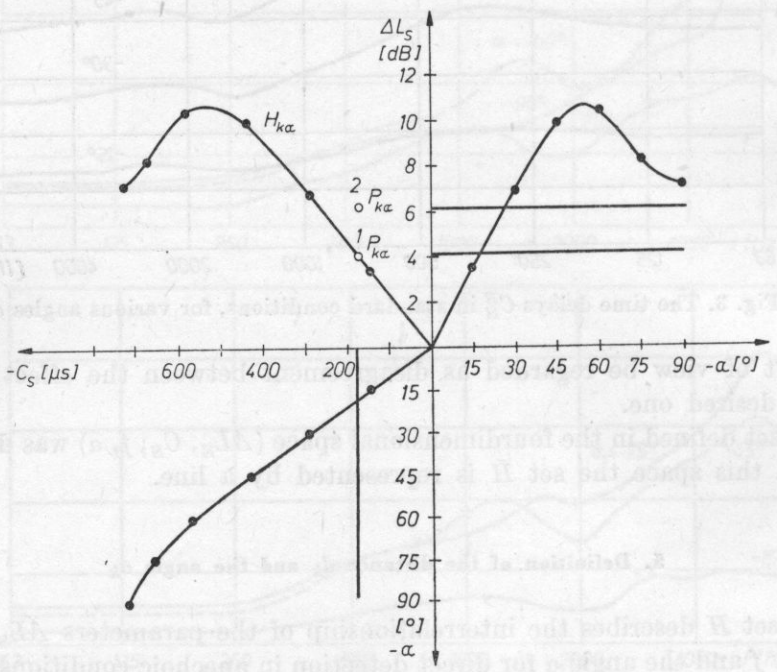

Fig. 4. Projections of the cross - section H_k and the straight lines ${}^1P_k$ and ${}^2P_k$ on the planes (ΔL_S,) C_S, (ΔL_S, α) and (C_S, α)

a spectrum - band with width df and the centre frequency f_k was considered. In standard conditions this band generates in the listener's ears $\Delta^1 L_{Sk}$ and ${}^1C_{Sk}$ — situation A, and with reflections from the walls, e.g. $\Delta^2 L_{Sk}$ and ${}^1C_{Sk}$ — — situation B. As a narrow frequency band is considered, analysis of these situations requires only the cross - section H_k of the set H for the frequency $f = f_k$. This cross - section can be represented in the space (ΔL_S, C_S, α). In the

threedimensional space, situations A and B are described by the parallel straight lines $(\Delta^1 L_{Sk}, {}^1C_{Sk}, \alpha)$ and $(\Delta^2 L_{Sk}, {}^1C_{Sk}, \alpha)$ called respectively ${}^1P_k$ and ${}^2P_k$ below. Fig. 4 shows the projections of the cross - section H_k and the straight lines ${}^1P_k$ and ${}^2P_k$ on the planes $(\Delta L_S, C_S)$, $(\Delta L_S, \alpha)$ and (C_S, α). The straight line ${}^1P_k$, corresponding to anechoic conditions, intersects the cross - section H_k at a point with the coordinates $(\Delta^1 L_{Sk}, {}^1C_{Sk}, \alpha_1)$ where the equation $\alpha_1 = \alpha_i$ is satisfied. In a general case the straight line ${}^2P_k$ has no common point with the cross - section H_k. In order to evaluate cases when the straight line describing a given situation has no common point with the cross - section H_k, the notion of distance was introduced. This will permit consideration of all possible interrelationships of the quantities ΔL_S, C_S, f and α.

The distance d_k^* of the straight line ${}^mP_k$ from the cross - section H_k of the set H is defined here as the distance between the rectangular projection of this straight line on the plane $(\Delta L_S, C_S)$ and the rectangular projection of the cross - section H_k on the same plane, where the level differences ΔL_S and the time delays C_S have been normalised.

The projection of the straight line ${}^mP_k$ on the plane $(\Delta L_S, C_S)$ is a point. Let ${}^mP_{k\alpha}$ denote this point. The projection of the cross - section H_k on the plane $(\Delta L_S, C_S)$ is a line. This line was designated as $H_{k\alpha}$. For a given frequency f_k the quantities ΔL_{Sk}^B are functions of the angle α, thus the coordinates of points lying on the line H_k depend on the angle α. It was assumed that there are the following normalising quantities:

– for the level difference ΔL_S – the number M_{Lk}, which is the maximum value of the level difference taken by the cross - section H_k for $\alpha \in (0, \pi/2)$,

– for the time delay C_S – the number M_{Ck}, which is the maximum value of the time delay taken by the cross - section H_k for $\alpha \in (0, \pi/2)$.

After normalisation the coordinates of the point ${}^mP_k$, (η_1, η_2), are as follows:

$$\eta_1 = \frac{\Delta^m L_{Sk}}{M_{Lk}}, \qquad \eta_2 = \frac{{}^mC_{Sk}}{M_{Ck}}. \tag{6}$$

In turn the coordinates of points lying on the line $H_{k\alpha}$, (λ_1, λ_2):

$$\lambda_1(\alpha) = \Delta L_{Sk}^B(\alpha)/M_{Lk}, \qquad \lambda_2(\alpha) = C_{Sk}^B(\alpha)/M_{Ck}. \tag{7}$$

The distance d_k^* can be determined from the relation

$$d_k^* \triangleq \min\{\varrho_k^*(\alpha)\}, \tag{8}$$

where

$$\varrho_k^*(\alpha) = \sqrt{[\eta_1 - \lambda_1(\alpha)]^2 + [\eta_2 - \lambda_2(\alpha)]^2}. \tag{9}$$

It should be borne in mind that in keeping with the definition the distance d_k^* is a number subordinated to the given frequency f_k.

The distance of the straight line ${}^mP_k$ from the cross-section H_k is conceived as a measure useful in determining the localisation direction of a sound source. Such a measure must in particular account for those properties of the human hearing organ that cause the time delay to have a decisive effect on source localisation at low frequencies and the level difference to do so at high frequencies. At medium frequencies the level difference and the time delay are equally essential [7, 18]. It is therefore necessary to introduce the weighted difference. After introducing the weight coefficients the definition of the distance becomes

$$d_k = \min\{\varrho_k(\alpha)\} = \min\left\{\sqrt{W_{Lk}(\eta_1-\lambda_1)^2+W_{Ck}(\eta_2-\lambda_2)^2}\right\}, \tag{10}$$

where W_{Lk} is the weight coefficient for ΔL_S for $f = f_k$; W_{Ck} is the weight coefficient for C_S for $f = f_k$.

At present there is no knowledge of the dependencies describing the properties of the human hearing organ as represented by the coefficients W_{Ck} and W_{Lk} in formula (10), except for their general trends. Therefore, it was assumed that they depended linearly on the logarithm of frequency and that they take values of zero or unity for frequencies of 16 Hz and 16.4 kHz giving the following expressions:

$$\begin{aligned} W_{Lk} &= 0.1\ \log_2 f_k - 0.4, \\ W_{Ck} &= -0.1\ \log_2 f_k + 1.4. \end{aligned} \tag{11}$$

The quantity α_k was also introduced. Let α_k denote an angle at which d_k occurs, i.e. α_k is such a value of the angle α at which the function $\varrho_k(\alpha)$ reaches a minimum. The quantity α_k is a function of the frequency f_k, just as so is the distance d_k.

6. Interpretation of the distance d_k and the angle α_k

As an example, Fig. 5 shows a projection of the cross-section H_k of the set H and projections of various possible straight lines ${}^mP_k$, marked by points A, B, C and D, on the plane (ΔL_S, C_S). Fig. 5 shows the cross-section of the set H determined in section 4 for $f_k = 1200$ Hz.

In situation A the straight line ${}^mP_k$ has a common point with the cross-section H_k. The distance d_k is zero. α_k is about -0.15π (-27^0). This situation can occur for direct detection in anechoic conditions, where there is the equation $\alpha_k = \alpha_i$ (α_i being the angle at which the sound source actually is). Situation A can also be generated by a signal transmitted by a stereophonic system. There is then full analogy to the standard conditions and it is not difficult to

determine the localisation direction of an image sound source. The listener evaluates that the image sound source is localised at the angle α_k. This stereophonic effect is a natural one.

In situation B in Fig. 5, the straight line ${}^mP_k$ has no common point with the cross-section H_k. However, the distance d_k is short ($d_k < d_g$, d_g — the limiting distance). The angle α_k is about -0.16π (-29^0). A situation such as B can be generated for direct detection in an interior with good acoustic condi-

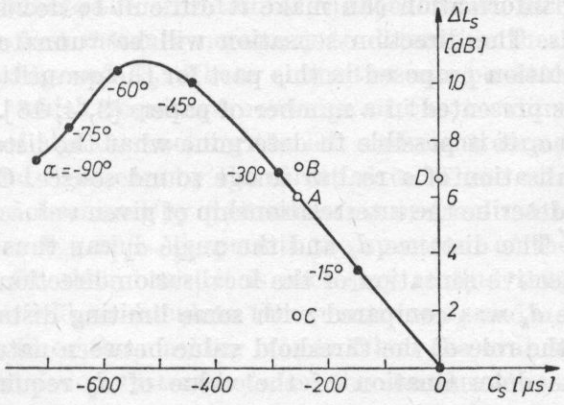

Fig. 5. Projections of the cross - section H_k and the straight lines ${}^mP_k$ on the plane (ΔL_S, C_S), $f_k = 1200$ Hz

tions. In such conditions, as a result of reflections from the walls of the interior reaching the listener's ears, there is a change (with respect to anechoic conditions) in the level difference ΔL_S. However, this change does not exceed 2 dB [10]. From psychoacoustic investigations, it follows that in such conditions localisation is good [11]. The angle at which the listener localises the sound source, is close to the angle α_i. Situation B can also be generated by a signal transmitted by a stereophonic system. It is then not difficult for the listener to determine the localisation direction of the image sound source.

In situation C the distance d_k is large ($d_k > d_g$).α_k is about -0.083π (-15^0). Situation C can be generated for direct detection in an interior with poor acoustic conditions [10]. In such conditions it is difficult, sometimes impossible, to localise, and the listener may evaluate wrongly the localisation of the sound source [13].

In situation D the distance d_k is also large ($d_k > d_g$). The angle α_k is about -0.11π (-20^0). Such a situation can occur for detection through a stereophonic system [10, 11]. Since the distance d_k (as in situation C) is large, the listener will find it difficult to determine the localisation direction of the sound source, as it is not important for the listener whether the given localisation parameters ΔL_{Sk} and C_{Sk} have been generated by signals reaching his ears directly from the source or through a stereophonic system.

The difficulties in determining the localisation direction of the sound source can be caused by "unnatural" interrelationships of the parameters of signals reaching the listener's ears, i.e. the frequency, the level difference ΔL_S and the time delay C_S. This can be an unnaturally large value of ΔL_S for a given frequency, e.g. for $f_k = 2$ kHz $\Delta L_{Sk} > 20$ dB, which in standard conditions does not occur for any angle α. This can be a zero value of the time delay C_{Sk} and a large value of ΔL_{Sk} at medium frequencies, for the zero time delay corresponds to the angle $\alpha = 0$, a large value of ΔL_S to a large negative angle α. The contradictory pieces of information can make it difficult to decide where the sound source actually is. The direction sensation will be "unnatural".

The interpretation proposed in this part for the quantities d_k and α_k agrees with observations presented in a number of papers [3, 4, 13]. With the distance d_k and the angle α_k it is possible to determine what the listener's decision will be as to the localisation of a real or image sound source. On the other hand, these quantities describe the interrelationship of given values of f, ΔL_{Sk} and C_{Sk} with the set H_k. The distance d_k and the angle α_k can thus be objective measures of the subjective sensation of the localisation direction of a sound source.

The distance d_k was compared with some limiting distance d_g. The latter distance played the role of the threshold value between natural and unnatural localisations. The determination of the value of d_g requires psychoacoustic investigations to be carried out. However, from the discussion given, it can be stated that localisation becomes more natural as the distance d_k decreases.

The above considerations are concerned with a narrow spectrum band with a centre frequency f_k of a signal emitted by a sound source. Since a source emits most frequently signals with composed spectrum, the determination of the listener's decision as to the localisation of the sound source, requires that d_k and α_k should be found for all the components of the spectrum of the signal detected by the listener. For direct detection in anechoic conditions, for all the spectral components the equation $\alpha_k = \alpha_i$ is satisfied, i.e. for all the components the source will be localised in its actual direction. At all frequencies the distance d_k will be zero. In evaluating the localisation of a real sound source in reverberation conditions, d_k will most frequently be non-zero and the angles α_k will be different from α_i. When the interior has good acoustic conditions, the distances d_k will be short, the angles α_k close to the angle α_i. As the acoustic conditions worsen d_k will increase and so will the scatter of the values of α_k about α_i. In determining the localisation direction of an image source, very diverse dependencies of α_k on frequency are possible (see Fig. 8). This depends above all on the way of transmitting the signal from the source to the listener's ears, i.e. on the properties of the stereophonic system [10, 11]. Therefore, in such a case, the use of the quantities d_k and α_k is a very useful way of evaluating the localisation sensation.

The interrelating, by means of the distance d_k and the angles α_k, of the

localisation parameters of signals reaching the listener's ears and the localisation sensation is the proposed criterion for evaluating the sensation of the localisation direction of a sound source.

7. Procedure of objective evaluation of the sensation of the localisation direction of a sound source

In order to evaluate the sensation of the localisation direction of a sound source, it is in the first instance necessary to determine the localisation parameters L_{SL}, L_{SL}, ΔL_S and C_S. These quantities can be determined from dependencies (1)-(4), which requires knowledge of the twodimensional autocorrelation functions of signals reaching the left and right ears and the delays in reaching the left and right ears by the direct wave. These correlation functions and delays can be determined by measurements or from mathematical models.

The parameters L_{SL} and L_{SP} permit the spectrum of the signal detected to be determined. On their basis, it is necessary to find the frequency bands for which it is justifield to calculate the quantities d_k and α_k, i.e. in terms of the hearing threshold or the masking effect. When the evaluation is to be carried out on a transmission system between the sound source and the listener's ears, the spectrum of the signal emitted by the source should cover all the frequency range under consideration.

In evaluating a stereophonic system it is also necessary to consider the effect of a later sound being masked by an earlier one. This phenomenon was described in paper [13]. As a result of investigations, it was established that when for a given time delay the level difference between signals emitted by two sound sources exceeds some threshold value, the sound source emitting the signal with the lower level will not be observed by the listener.

Having definite localisation parameters ΔL_S and C_S and using a decision-making model represented by the set H, the distances d_k and the angles α_k should be determined for particular spectrum bands. Subsequently on the basis of d_k and α_k it is possible to carry out an objective evaluation of a given localisation sensation. The direction sensation improves as the angles α_k show less and less scatter about some mean value and as the distances d_k decrease. In addition, in evaluating the direction sensation generated by means of a stereophonic system, it should be considered whether the system provides the possibility of the image sound source being localised at any point of the base.

Apart from their dependence on frequency, the localisation parameters ΔL_S and C_S, and thus accordingly the quantities d_k and α_k, depend on a large number of other factors. In the case of a stereophonic system the localisation parameters are affected by such factors as the angles at which sound sources are localised with respect to the microphones, the characteristics of the micro-

phones and loudspeakers, the parameters describing reflections from the walls etc. [10, 11]. Thanks to the method proposed, the effect exerted by all of these factors on localisation can be analysed thoroughly.

8. Evaluation of a two-channel loudspeaker intensity stereo-system

Using the mathematical model of the stereophonic system under consideration [10, 11], on the assumption that: the detecting and transmitting interiors are anechoic in character, the stereophonic system is a symmetrical one, the microphones making up the coincidence microphone have cardioidal characteristics, the angle of the base is $\pi/2$ and that the source emits a signal described by the autocorrelation function $R_{xx}(t_1, t_2) = {}^2\delta(t_1, t_2)$, the localisation parameters were calculated. Because of the symmetry assumed for the stereophonic system, the time delay C_s is zero by identity. The dependence of the level difference ΔL_S on frequency for some angles at which the sound source is localised with respect to the coincidence microphone (the angle φ), is shown in Fig. 6.

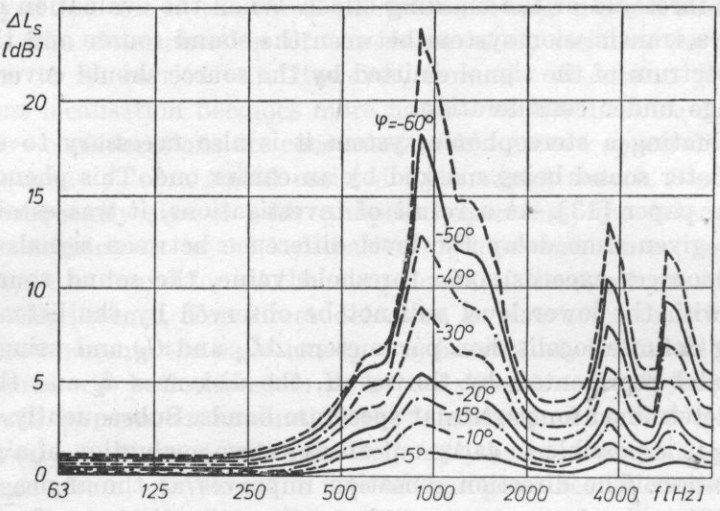

Fig. 6. Differences in the short - term spectral power levels, ΔL_S, for the chosen version of two - channel loudspeaker intensity stereophony, for various angles α

Subsequently, in keeping with the procedure shown in section 7, the distances d_k and the angles α_k were calculated. The results of the calculations are given in Figs. 7 and 8. On the basis of these results and those of calculations carried out for other variants of two-channel loudspeaker intensity stereosystem [10], it was established that:

— for the angles $\varphi \in (-\pi/6, \pi/6)$ at which the sound source is localised with respect to the microphone, the stereophonic system ensures such a representa-

tion in which the larger angle φ corresponds to the larger angle α_k at which the image sound source is situated with respect to the listener. As a result of this, there occurs the sensation of a "blurred" sound source emitting composed spectra. A point sound source will occupy part of the base,

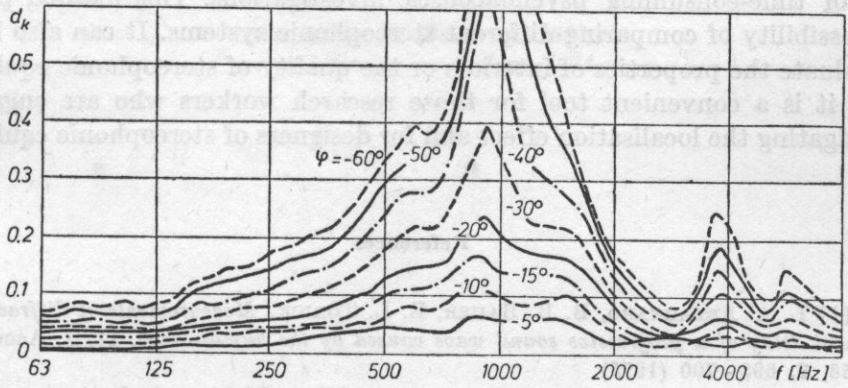

Fig. 7. The calculated distances d_k

— when the sound source emits a signal whose spectrum will be concentrated about some frequency, the image source changes its position on the base as this frequency varies,

— when the sound source emits a low-frequency signal, the image sound source is localised close to the centre of the base,

— in limited frequency bands image sound sources are localised beyond the base section.

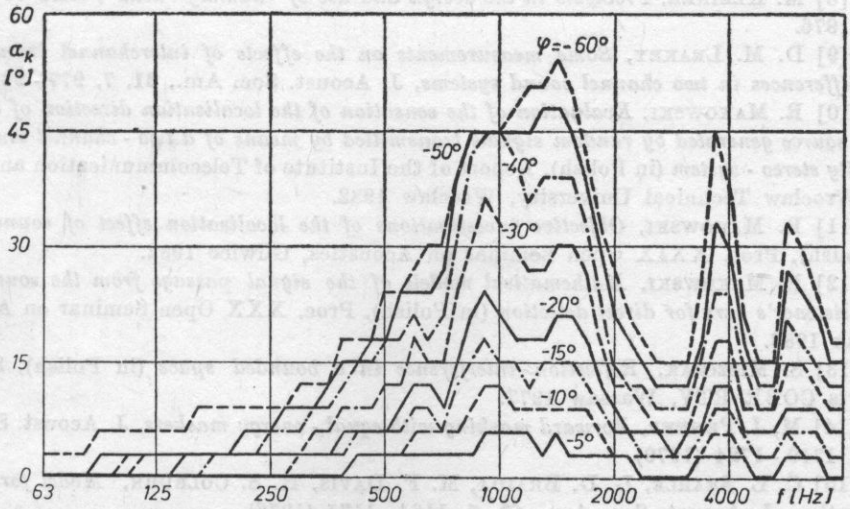

Fig. 8. The angles α_k of the localisation of the image sound source with respect to the listener

9. Conclusion

The method proposed represents a new approach to the evaluation of the localisation effect, permitting this evaluation to be carried out without the need of time-consuming psychoacoustic investigations. This method provides the possibility of comparing different stereophonic systems. It can also be used to evaluate the properties of interiors or the quality of stereophonic equipment. Thus, it is a convenient tool for those research workers who are engaged in investigating the localisation effect and for designers of stereophonic equipment.

References

[1] L. A. ABBAGNARO, B. B. BAUER, E. L. TORICK, *Measurements of diffraction and interaural delay of a progressive sound wave caused by the human head.* II, J. Acoust. Soc. Am., **58**, 3, 693 - 700 (1975).

[2] B. BERNFELD, B. SMITH, *Computer - aided model of stereophonic systems*, 59 th Convention AES, Hamburg 1978.

[3] J. BLAUERT, *Räumliches hören*, S. Hirzel Verlag, Stuttgart, 1974.

[4] V. V. FURDUEV, *Stereofonia: mnogokanalnye zvukovye sistemy*, Energia, Moscow 1973.

[5] M. GŁABISZ, B. W. KULESZA, R. SZKOP, *An acoustic model of an artificial head for the investigation of stereophonic systems* (in Polish), Archiwum Akustyki, **15**, 2, 191 - 198 (1980).

[6] H. HAAS, *Über den Einfluss eines Einfachechos auf die Hörsamkait von Sprache*, Acustica, **1**, 1, 49 - 65 (1951).

[7] G. H. HENNING, *Detectability of interaural delay in high - frequency complex waveforms*, J. Acoust. Soc. Am., **55**, 1, 84 - 90 (1974).

[8] M. KLEINER, *Problems in the design and use of "dummy - head"*, AES 75 Convention, 1976.

[9] D. M. LEAKEY, *Some measurements on the effects of interchannel intensity and time differences in two channel sound systems*, J. Acoust. Soc. Am., **31**, 7, 977 - 986 (1959).

[10] R. MAKOWSKI, *Evaluation of the sensation of the localisation direction of an image sound source generated by random signals transmitted by means of a two - channel loudspeaker intensity stereo - system* (in Polish), Report of the Institute of Telecommunication and Acoustics, Wrocław Technical University, Wrocław 1982.

[11] R. MAKOWSKI, *Objective investigations of the localisation effect of sound sources* (in Polish), Proc. XXIX Open Seminar on Acoustics, Gliwice 1982.

[12] R. MAKOWSKI, *Mathematical models of the signal passage from the sound source to the listener's ears for direct detection* (in Polish), Proc. XXX Open Seminar on Acoustics, Gdańsk 1983.

[13] S. MISZCZAK, *Reflection interference in a bounded space* (in Polish), Scientific Reports COBR RTV, Warsaw 1977.

[14] M. J. PENNER, *Forward masking with equal - energy maskers*, J. Acoust. Soc. Am., **66**, 6, 1719 - 1724 (1979).

[15] C. L. SEARLE, L. D. BRAIDA, M. F. DAVIS, H. S. COLBURN, *Model for auditory localization*, J. Acoust. Soc. Am., **60**, 5, 1164 - 1175 (1976).

[16] E. A. G. SHAW, *Earcanal pressure generated by a free sound field*, J. Acoust. Soc. Am., **39**, 3, 465 - 470 (1966).

[17] E. A. G. SHAW, *Transformation of sound pressure level from the free field to eardrum in the horizontal plane*, J. Acoust. Soc. Am., **56**, 6, 1848 - 1861 (1974).

[18] Z. ŻYSZKOWSKI, *Fundamentals of electroacoustics* (in Polish), WNT, Warsaw 1966.

Received on 17 February, 1983;
revised version on 7 June 1984.

ARCHIVES OF ACOUSTICS
9, 4, 291-304 (1984)

A VIBROACOUSTIC MODEL OF A REDUCTION LINE OF A GAS INSTALLATION

ZBIGNIEW ENGEL, RYSZARD PANUSZKA

Institute of Mechanics and Vibroacoustic of the Academy of Mining and Metallurgy
(30 - 059 Cracow, al. Mickiewicza 30)

MIECZYSŁAW MENŻYŃSKI

Carpathian District Gas Plant
(33 - 100 Tarnów, ul. Nowy Świat 78)

This paper proposes a method for predicting the sound power level of a reduction line of a gas installation, based on a vibroacoustic cylindrical equivalent model. This model was verified experimentally on a real object. It permits approximate prediction of the sound power level of a reduction line, depending on its technological and structural parameters, particularly for medium and high frequencies.

1. Introduction

Prediction of the value of sound power radiated by sound sources on machinery and industrial facilities is one of the essential problems in machinery vibroacoustics. Attempts to develop methods for predicting the values of the power level of sound sources were undertaken for plates in the case of flexural resonance vibration [2] and for pipes involving turbulent water flow [1, 6].

The present authors are concerned with the problem of predicting values of the sound power radiated by sources with complex geometry, such as occur in gas pipelines. The considerations apply only to radiation of sound power by surface sources [8].

The principal object of this paper is to build and verify experimentally a model of radiation by a system of sound sources with complex geometry, where acoustic energy radiation is caused by gas flow in the process of pressure reduction. This purpose was carried out by forming an equivalent cylindrical

radiation model. It is assumed that the velocity of radial vibration of the walls of the line is a function of the gas flow intensity. This assumption was verified experimentally.

2. Acoustic model of the line

In building the acoustic equivalent model of the line, elements with complex geometry were replaced by cylindrical ones with equivalent surface area and length equal to the linear dimension of a given element, measured along the axis of the line. A system of cylindrical sources thus formed was replaced by one cylindrical source with the length of the real line and an equivalent diameter (Fig. 1). The assumption of the equivalent model of the line in the form of a cylindrical source was based on the acoustic field distribution as published in papers [3, 4].

In modelling the following assumptions were made:

– the emission of acoustic energy outside a cylinder with infinite length, vibrating stochastically and stationarily over a broad frequency range, is considered;

– the surface of the cylinder vibrates in the radial mode;

– the frequency range $\Delta f = 500\text{-}8000$ Hz;

– there is critical flow in the reductor valve ($\beta = p_2/p_1 < 0.542$, where p_1 and p_2 are the values of the pressures occurring before and behind the reductor, respectively).

The cylindrical acoustic model of the line is replaced by a system of rectangular pistons with dimensions $2z_0$ and $2a$ (Fig. 2), separated on its side surface and vibrating with equal amplitude and phase. It is assumed that the motion of the pistons is not correlated. Hence, the mean square values of the acoustic pressures and the sound power radiation intensity in the field outside the side surface of the cylinder are approximately proportional to the sum of the mean square values of the pressures generated successively by each of the pistons vibrating in an infinite cylindrical baffle.

LAIRD and COHEN [7] derived the expression for the acoustic pressure in a point in the far field with the coordinates R, Φ, θ (Fig. 3), in the form

$$p = 2\varrho c v_r P \exp[j(kR - 2\pi ft)], \tag{1}$$

where ϱ is the density of the medium, c-the acoustic velocity, v_r – the amplitude of the radial component of the velocity of the piston, k – the wave number, and P is expressed by the relation

$$P = \frac{1}{\pi kR} \frac{\sin(kz_0 \cos\theta)}{\cos\theta \sin\theta} \left\{ \left(\frac{a}{\pi}\right) \frac{1}{H_0^{(1)'}(ka_{eq} \sin\theta)} + \right.$$
$$\left. + \sum_{m=1}^{\infty} \left[\frac{2\sin m\alpha}{m\pi} \frac{\exp(-jm\pi/2)}{H_m^{(1)'}(ka_{eq} \sin\theta)} \right] \times \cos m\Phi \right\}. \tag{2}$$

In this expression, a_{eq} is the equivalent radius of the cylinder, $H_0^{(1)'}$ is the derivative of a Hankel function of the zeroth order, of the first kind, $H_m^{(1)'}$ — — the derivative of a Hankel function of the mth order, of the 1st kind.

Subsequently, KENNEDY and YOUNG [6] determined the intensity of sound power radiation in the radial direction from the product

$$\frac{1}{2}(2\varrho c v_r P)(2v_r \sin\theta P^*),$$

where P^* is a complex conjugate of P.

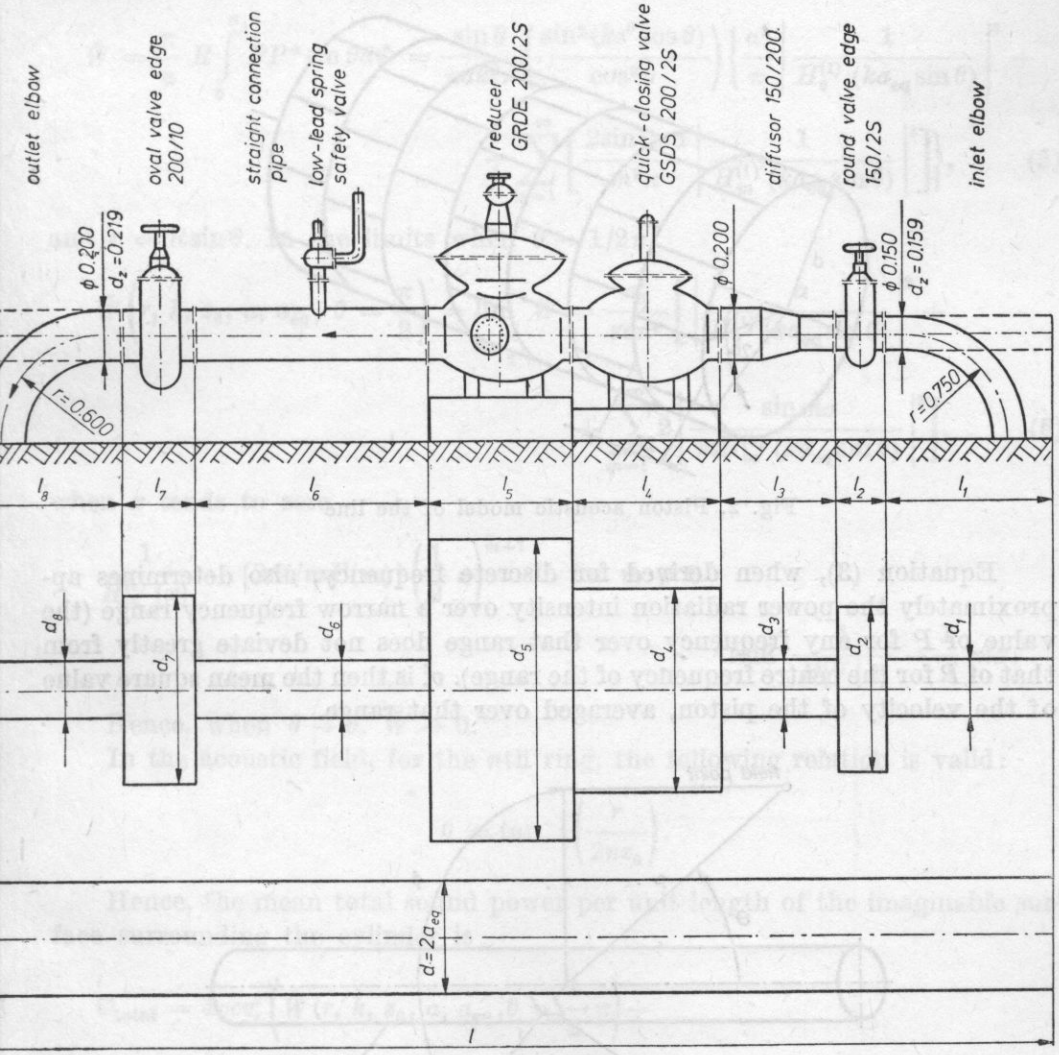

Fig. 1. Procedure of the stage transition from the real object to the equivalent cylindrical model of the line. The values are given in m

Taking the imaginable cylindrical surface with the radius $r = R\sin\theta$, parallel and concentric with the cylindrical baffle, the total sound power radiation intensity in the radial direction, corresponding to unit length, is

$$\overline{w} = 2\int_0^{\pi} \frac{1}{2}(2\varrho c v_r P)(2v_r \sin\theta P^*) R\sin\theta d\Phi =$$

$$= 4\varrho c v_r^2 R \int_0^{\pi} PP^* \sin\theta d\Phi \,[Wm^{-2}]. \qquad (3)$$

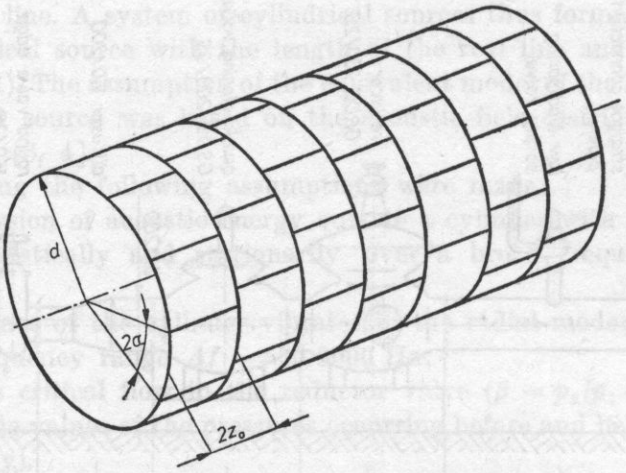

Fig. 2. Piston acoustic model of the line

Equation (3), when derived for discrete frequency, also determines approximately the power radiation intensity over a narrow frequency range (the value of P for any frequency over that range does not deviate greatly from that of P for the centre frequency of the range). v_r^2 is then the mean square value of the velocity of the piston, averaged over that range.

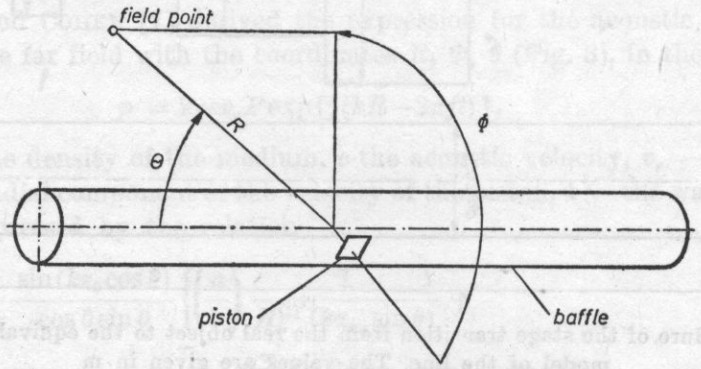

Fig. 3. Piston model of the line in a cylindrical coordinate system

The total power radiation intensity is equal to the sum of the radiation power densities of particular vibrating pistons. The system of the pistons is defined by an infinite series of rings with the axial length $2\,z_0$. Each of the rings contains about π/a pistons, hence the sound power radiated by all the pistons in the first ring is

$$\overline{w} = \left(\frac{\pi}{a}\right) w = 4\varrho c v_r^2\, \tilde{W}(r, k, z_0, a, \theta, a_{eq}) \quad [\mathrm{W}], \tag{4}$$

where

$$\tilde{W} = \frac{\pi}{a} R \int_0^{\pi} PP^* \sin\theta d\Phi = \frac{\sin\theta}{\pi a k^2 r}\left(\frac{\sin^2(kz^0\cos\theta)}{\cos^2\theta}\right)\left\{\frac{a^2}{\pi}\left|\frac{1}{H_0^{(1)'}(ka_{eq}\sin\theta)}\right|^2 + \right.$$

$$\left. + \sum_{m=1}^{\infty}\left[\frac{2\sin^2 ma}{m^2\pi}\left|\frac{1}{H_m^{(1)'}(ka_{eq}\sin\theta)}\right|^2\right]\right\}, \tag{5}$$

and $r = R\sin\theta$. In the limits when $\theta \to 1/2\pi$

$$\tilde{W}\left(r, k, z_0, a, a_{eq}, \theta = \frac{\pi}{2}\right) = \lim_{\theta\to\frac{\pi}{2}} \tilde{W} = \frac{z_0^2}{ra\pi^2}\left[\left|\frac{a}{H_0^{(1)'}(ka_{eq}\sin\theta)}\right|^2 + \right.$$

$$\left. + \sum_{m=1}^{\infty} 2\left|\frac{\sin ma}{mH_m^{(1)'}(ka_{eq}\sin\theta)}\right|^2\right], \tag{6}$$

when x tends to zero

$$\frac{1}{H_m^{(1)'}(x)} - \{2\pi i/m\Gamma(m)\}\left(\frac{1}{2}x\right)^{m+1} \quad \text{for } m \neq 0$$

$$\text{and } \frac{1}{H_0^{(1)'}(x)} \to \frac{1}{2}\pi i x.$$

Hence, when $\theta \to 0$, $\tilde{W} \to 0$.

In the acoustic field, for the nth ring, the following relation is valid:

$$\theta = \tan^{-1}\left(\frac{r}{2nz_0}\right).$$

Hence, the mean total sound power per unit length of the imaginable surface surrounding the cylinder is

$$\overline{w}_{\text{total}} = 4\varrho c v_r^2\left(\tilde{W}(r, k, z_0, a, a_{eq}, \theta = \frac{1}{2}\pi) + \right.$$

$$\left. + 2\sum_{n+1}^{\infty}\tilde{W}\left[r, k, z_0, a, a_{eq}, \theta = \tan^{-1}\left(\frac{r}{2nz_0}\right)\right]\right). \tag{7}$$

The expression $2\sum_{n=1}^{\infty}\tilde{W}[r, k, z_0, a, a_{eq}, \theta = \tan^{-1}(r/2nz_0)]$ can be approximated, when $r \to \infty$, by the relation [6]

$$\int_0^{\pi/2} \frac{r}{z_0 \sin^2\beta}\, \tilde{W}(r, k, z_0, a, a_{eq}, \beta)\, d\beta. \tag{8}$$

It follows from equations (5) and (6) that the first term of equation (7) is inversely proportional to r. The remainder of the expression is given by equation (8) and does not depend on r within the interval $0 \leqslant \beta \leqslant 1/2\pi$. Because the first term of equation (7) is inversely proportional to r and the summary term does not depend on r, for sufficiently large values of r the first term can be neglected.

With $Z = z_0/\lambda$ and $A = -a_{eq}/\lambda$, where λ is the wave length, the following expression for sound power can be derived from equations (7) and (8),

$$\overline{w}_{total} = \varrho c v_r^2 \lambda I(a, Z, A) \quad [\mathrm{W}], \tag{9}$$

where

$$I = \frac{1}{\pi^4 a z_0} \int_0^{\pi/2} \frac{\sin^2(2\pi Z \cos\beta)}{\cos^2\beta \sin\beta} \left\{ \left| \frac{a}{H_0^{(1)'}(2\pi A \sin\beta)} \right|^2 + \right.$$

$$\left. + \sum_{m=1}^{\infty} \left[\frac{2\sin^2 m a}{m^2} \left| \frac{1}{H_m^{(1)'}(2\pi A \sin\beta)} \right|^2 \right] \right\} d\beta. \tag{10}$$

Fig. 4 shows the characteristic of log I as a function of the quantity A, as determined by KENNEDY and YOUNG [6].

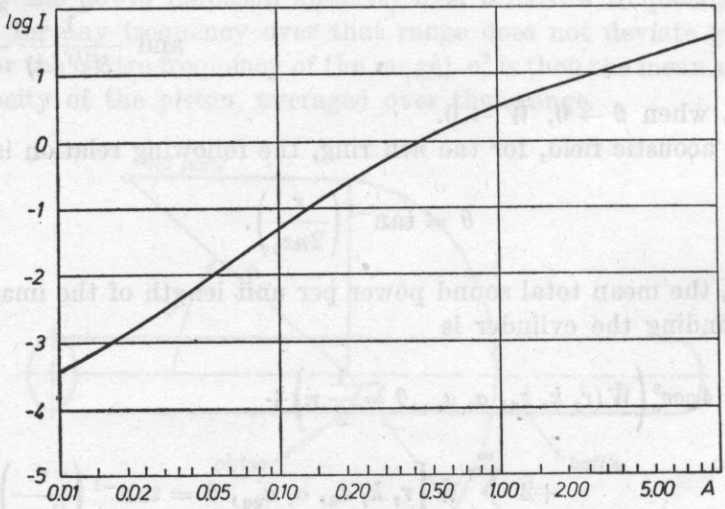

Fig. 4. Curve of log I as a function of the quantity A

Equation (9) was derived for an infinitely long system of pistons vibrating in a cylindrical baffle. In the case of a long pipe with finite length l[m] ($l/a_{eq} \gg 1$), for which the diffraction phenomena at its ends can be neglected, the theoretical sound power level L_{Wt} radiated for $\varrho c = 428.6$ Nsm^{-3} can be expressed approximately by the relation

$$L_{Wt} = 10\log\frac{\overline{w}_{\text{total}}}{W_0} l = 146 + 20\log\bar{v}_r + 10\log\lambda + 10\log I \quad [\text{dB}], \tag{11}$$

where $W_0 = 10^{-12}$[W] is the reference power level, λ - the wave length [m], log I is the value determined from the curve in Fig. 4, v_r[ms^{-1}] - the mean value of the velocity of radial vibration.

3. Vibrating model of the line

The acoustic model makes the mean sound power $\overline{W}$ radiated dependent on the value of the mean radial vibration velocity of the walls of the line, $\bar{v}_r$, according to the function

$$\overline{W} = \varphi_1(\bar{v}_r, f, a_{eq}, l) \quad [\text{W}]. \tag{12}$$

In the vibration model, the mean value of the radial vibration velocity of the walls of the reduction line, $\bar{v}_r$, depends on the gas flow intensity Q[m^{3}h^{-1}], the vibration frequency f[Hz], the equivalent radius a_{eq}[m] and the length l[m], according to the function

$$\bar{v}_r = \varphi_2(Q, f, a_{eq}, l) \quad [\text{m}\cdot\text{s}^{-1}]. \tag{13}$$

The vibration model and the acoustic one, which form together a vibroacoustic model, are shown in Fig. 5.

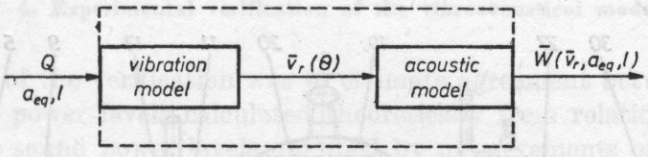

Fig. 5. Schematic diagram of the vibroacoustic equivalent model of the line

The function given by relation (13) can be determined by investigations performed on real lines. In the case of a set of K lines, it is possible to derive the functions

$$v_{rK} = \varphi_k(Q, f), \tag{14}$$

where a_{eq}, l = const.

Hence, the mean function is sought:

$$\bar{v}_r = \bar{\varphi}(Q, f), \tag{15}$$

where

$$Q[Q_{\min}, Q_{\max}], \varphi[f_{\min}, f_{\max}]. \tag{16}$$

The flow intensity Q varies in time. Assuming that the discrete values of the flow intensity, Q_{K_i}, are known for particular lines, the function Q_K can be written as

$$Q_K = Q_{\text{VAR}}[Q_{K_1}, Q_{K_2}, \ldots, Q_{K_i} \ldots, Q_{K_m}], \tag{17}$$

where $m = 1, 2 \ldots$ are discrete values of the gas flow intensity Q_K.

For each of the lines, the mean value of the function is determined from (13) by averaging

$$\bar{v}_{r_K} = \sqrt{\frac{1}{n} \sum_{i=1}^{n} v_{r_i}^2}, \tag{18}$$

where n is the number of points for the measurement of the radial vibration velocity on the line. Hence, the mean value of the function of the radial vibration velocity can be determined in the form

$$\bar{v}_r(Q, f) = \frac{1}{K} \sum_{i=1}^{K} v_{r_K} \quad [\text{ms}^{-1}]. \tag{19}$$

The function given by relation (13) was determined experimentally on 3 lines with the first degree of pressure reduction, in the same technological and structural system, as shown in Fig. 1.

The investigations were carried out for gas flow intensities contained within the interval (2315-6480) m^3h^{-1} under normal conditions. The distribu-

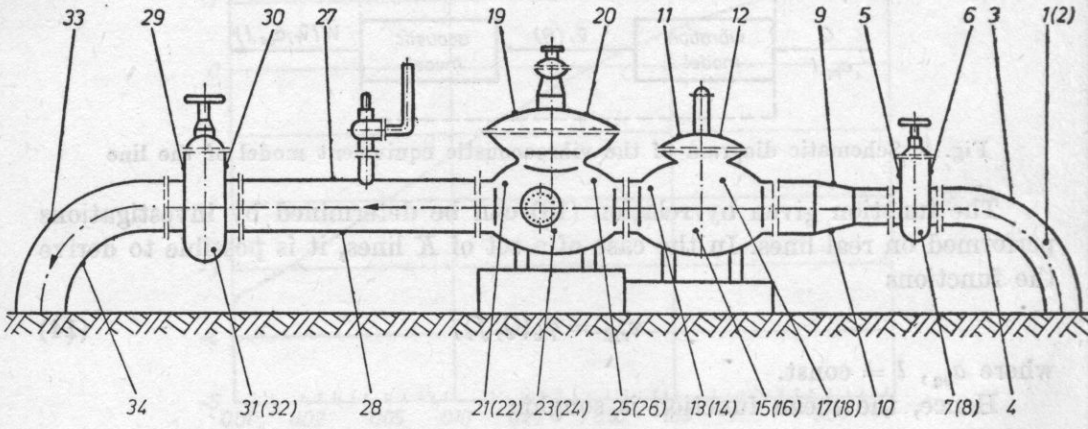

Fig. 6. Distribution of the measurement points on the surface of the line

tion of the measurement points on the surfaces of the particular elements is shown in Fig. 6. In turn, Fig. 7 gives the mean values of the amplitudes of the radial vibration velocity of the line, as obtained from relation (19). They are the basis for determination of the sound power level radiated by the reduction line.

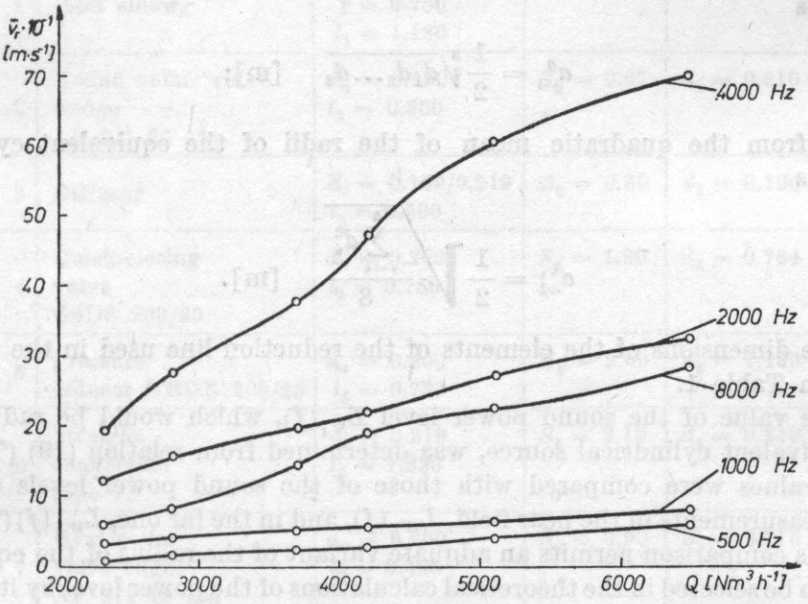

Fig. 7. Characteristics of the mean values of the radial vibration velocities as a function of the gas flow intensity

4. Experimental verification of the vibroacoustical model

The aim of the verification was to estimate agreement between the values of the sound power levels calculated theoretically from relation (11) and the values of the sound power levels obtained by measurements on a real object. The investigations were based on the sound pressure level distributions in the near and far fields which were given in papers [3] and [4].

In the theoretical calculations, four variant ways of averaging the radius of the equivalent cylinder, a_{eq} were employed:

— from the total real surface area of the elements of the line

$$a_{eq}^{c} = \frac{S}{2\pi l} \quad [\mathrm{m}]; \tag{20}$$

— from the arithmetic mean of the radii of the equivalent cylindrical ele-

ments

$$a_{eq}^{a} = \frac{\sum_{i=1}^{8} d_i}{2 \cdot 8} \quad [\mathrm{m}]; \tag{21}$$

– from the geometric mean of the radii of the equivalent cylindrical elements

$$a_{eq}^{g} = \frac{1}{2} \sqrt[8]{d_1 d_2 \ldots d_8} \quad [\mathrm{m}]; \tag{22}$$

– from the quadratic mean of the radii of the equivalent cylindrical elements

$$a_{eq}^{k} = \frac{1}{2} \sqrt{\frac{\sum_{i=1}^{8} d_i^2}{8}} \quad [\mathrm{m}]. \tag{23}$$

The dimensions of the elements of the reduction line used in the tests are listed in Table 1.

The value of the sound power level $L_{W_t}(f)$, which would be radiated by the equivalent cylindrical source, was determined from relation (19) (Table 2). These values were compared with those of the sound power levels obtained from measurements in the near field, $L_{W_b}(f)$, and in the far one, $L_{W_d}(f)$ (Table 3).

This comparison permits an adquate variant of the radius of the equivalent model to be selected in the theoretical calculations of the power level by its experimental verification. For this purpose, for the four variants of the radius assumed, calculations were carried out of the theoretical level of the total sound power radiated over the five frequency ranges under study, according to the dependence

$$L_{W_t} = 10 \log \frac{\sum_{i=1}^{5} W_{i_t}(f_i)}{W_0} \quad [\mathrm{dB}], \tag{24}$$

where $W_{i_t}(f_i)$ [W] is the sound power of the line over the 1/3 octave band with the centre frequency f_i, determined theoretically.

Similar calculations of the total sound power levels were carried out for the near and far fields, according to the dependencies

$$L_{W_b} = 10 \log \frac{\sum_{i=1}^{5} W_{i_b}(f_i)}{W_0} \quad [\mathrm{dB}], \tag{25}$$

$$L_{W_d} = 10 \log \frac{\sum_{i=1}^{5} W_{i_d}(f_i)}{W_0} \quad [\mathrm{dB}], \tag{26}$$

Table 1. Dimensions of the line

No	Element	Real dimensions [m]	Surface area [m²]	Equivalent cylinder diameter [m]
1	Inlet elbow	$d_z = 0.159$ r = 0.750 $l_1 = 1.180$	$S_1 = 0.59$	$d_1 = 0.159$
2	Round collar valve wedge AP 5/1 25 atn	$d_n = 0.150$ $l_2 = 0.350$	$S_2 = 0.67$	$d_2 = 0.610$
3	Diffusor	$d_z = 0.159/0.219$ $l_3 = 0.500$	$S_3 = 0.30$	$d_3 = 0.190$
4	Quick-closing valve GSDS 200/25	$d_n = 0.200$ $l_4 = 0.750$	$S_4 = 1.80$	$d_4 = 0.764$
5	Pressure reducer GRDE 200/25	$d_n = 0.200$ $l_5 = 0.720$	$S_5 = 2.60$	$d_5 = 1.149$
6	Straight connection pipe	$d_z = 0.219$ $l_6 = 1.830$	$S_6 = 2.16$	$d_6 = 0.219$
7	Oval collar valve edge AP 5/1 10 atn	$d_n = 0.200$ $l_7 = 0.400$	$S_7 = 0.90$	$d_7 = 0.716$
8	Outlet elbow	$d_z = 0.219$ $r = 0.600$ $l_8 = 0.950$	$S_8 = 0.65$	$d_8 = 0.219$
9	Whole line	$d_n = 0.200$ $l = 6.680$	$S = 8.77$	$d = 0.418$

where $W_{i_b}(f_i)$ [W] is the sound power of the line in the 1/3 octave band with the centre frequency f_i, determined in the near field; and $W_{i_d}(f_i)$ [W] is the sound power of the line in the 1/3 octave band with the centre frequency f_i determined in the far field.

The differences among the values of the total sound power levels calculated from (24-26) were determined according to the dependencies

$$\Delta L_{W_1} = L_{W_t} - L_{W_b} \quad [\text{dB}], \tag{27}$$

$$\Delta L_{W_2} = L_{W_t} - L_{W_d} \quad [\text{dB}]. \tag{28}$$

Table 4 lists the calculated values of the total sound power levels and their differences. It follows from this table that the least difference among the

Table 2. Calculated values for determination of the theoretical sound power level of a reduction line

Centre frequency of 1/3 octave band f [Hz]	Radial vibration velocity $\bar{v}_r 10^{-4}$ [m s^{-1}]	$20 \log \bar{v}_r$	Line length l [m]	$10 \log l$	Wave length λ [m]	$10 \log I$	Line model radius a [m]	$A = a/\lambda$	$\log I$	$10 \log I$	Theoretical sound power level $L_{Wl}(f)$ [dB]
500	5.6	−65.0	6.680	8.2	0.663	−1.8	$a_c = 0.209$	0.31	−0.30	−3.0	84.4
							$a_a = 0.252$	0.38	−0.15	−1.5	85.9
							$a_g = 0.196$	0.29	−0.35	−3.5	83.9
							$a_k = 0.303$	0.46	0.00	0.0	87.4
1000	7.7	−62.3			0.331	−4.8	$a_c = 0.209$	0.63	0.20	2.0	89.1
							$a_a = 0.252$	0.76	0.35	3.5	90.6
							$a_g = 0.196$	0.59	0.15	1.5	88.6
							$a_k = 0.303$	0.91	0.45	4.5	91.6
2000	32.2	−49.8			0.165	−7.8	$a_c = 0.209$	1.27	0.60	6.0	102.6
							$a_a = 0.252$	1.53	0.70	7.0	103.6
							$a_g = 0.196$	1.19	0.55	5.5	102.1
							$a_k = 0.303$	1.84	0.75	7.5	104.1
4000	69.7	−43.1			0.083	−10.8	$a_c = 0.209$	2.52	0.90	9.0	109.3
							$a_a = 0.252$	3.04	1.00	10.0	110.3
							$a_g = 0.196$	2.36	0.85	8.5	108.8
							$a_k = 0.303$	3.65	1.05	10.5	110.8
8000	27.7	−51.1			0.041	−13.9	$a_c = 0.209$	5.10	1.20	12.0	101.2
							$a_a = 0.252$	6.15	1.30	13.0	102.2
							$a_g = 0.196$	4.78	1.15	11.5	100.7
							$a_k = 0.303$	7.39	1.35	13.5	102.7

Table 3. Levels of averaged sound pressures and sound powers of the whole reduction line in the near and far fields

Level [dB]	Centre frequency of 1/3 octave band [Hz]				
	500	1000	2000	4000	8000
$^{L}P_{avb}$	69.5	79.8	93.9	98.4	92.6
$^{L}W_b$	78.9	89.2	103.3	107.8	102.0
$^{L}P_{avd}$	62.8	78.0	86.2	94.1	87.7
$^{L}W_d$	80.2	95.4	103.6	111.5	105.1

results obtained, both for the far and the near fields, occurs in the case of assuming in theoretical calculations the radius a^{g}_{eq}.

Fig. 8 represents graphically comparison between the theoretically determined sound power levels with those measured in the near and far fields. The behaviour of these levels indicates that at low frequencies deviations occur

Table 4. Measured values of the sound power levels of the line

Variant of equivalent radius	Total power level at frequencies under study			Differences in total power levels	
	$^{L}W_t$[dB]	$^{L}W_b$[dB]	$^{L}W_d$[dB]	$^{L}W_1$[dB]	$^{L}W_2$[dB]
a^{c}_{eq}	110.7	109.9	110.0	0.8	0.7
a^{a}_{eq}	111.7			1.8	1.7
a^{g}_{eq}	110.2			0.3	0.2
a^{k}_{eq}	112.2			2.3	2.2

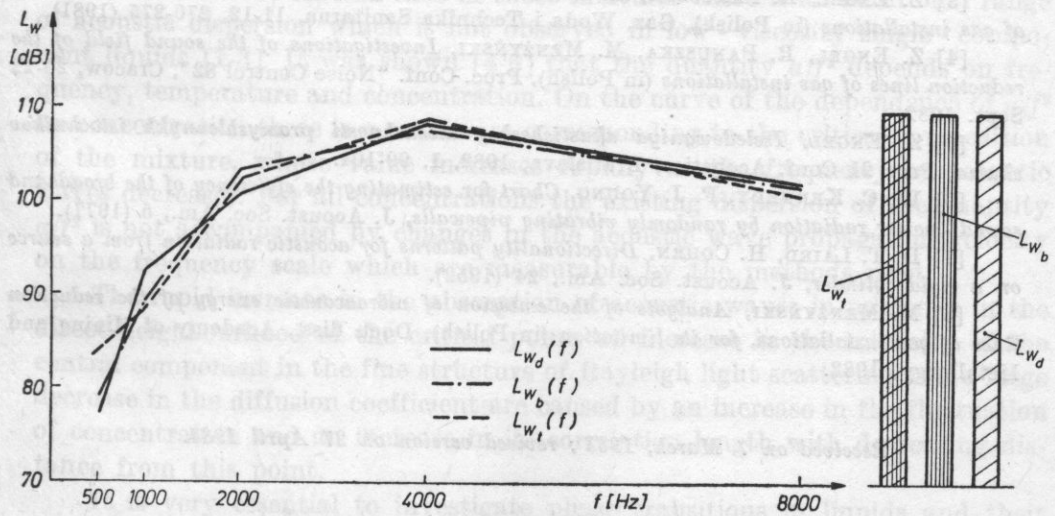

Fig. 8. Comparison of the determined sound power levels for the line

(being maximum, of about 7 dB, in the band of 500 Hz). At higher frequencies, however, (2000-8000 Hz), i.e. where characteristically of the reduction line maximum level values occur, there is agreement among the results obtained, likewise in total sound power levels. This agreement confirms the validity of the method assumed for selection of the equivalent model of the reduction line.

5. Conclusions

The results of the experimental investigations of the spatial distribution of the sound field of the reduction line served to build an equivalent vibroacoustic model of the line and for its experimental verification.

This equivalent vibroacoustic model permits approximate prediction of the sound power level of a reduction line, depending on its technological and structural properties, with the best results being obtained for medium and high frequencies.

The method proposed here for the construction of the equivalent model was verified for lines with the nominal diameter $d_n = 0.2$ m; it can also be used to build equivalent models of lines with different parameters.

References

[1] J. M. CLINCH, *Prediction and measurement of the vibrations induced in thin - walled pipes by the passage of internal turbulent water flow*, JSV, 12 (1970).

[2] S. CZARNECKI, Z. ENGEL, R. PANUSZKA, *Sound power and radiation efficiency of a circular plate*, Archives of Acoustics, **1**, 3, 201-213 (1976).

[3] Z. ENGEL, R. PANUSZKA, M. MENŻYŃSKI, *Noise propagation by technological lines of gas installations* (in Polish), Gaz, Woda i Technika Sanitarna, 11-12, 270-275 (1981).

[4] Z. ENGEL, R. PANUSZKA, M. MENŻYŃSKI, *Investigations of the sound field of the reduction lines of gas installations* (in Polish), Proc. Conf. "Noise Control 82", Cracow, 20-22 Sept. 1982.

[5] Z. ENGEL, *Issledowaniya akusticheskoy moshchnosti promyshlennykh istochnikov shuma*, Proc 21 Conf. Acoustics, Bratislava, 1982, **1**, 99-104.

[6] W. C. KENNEDY, F. J. YOUNG, *Chart for estimating the efficiency of the broadband sound - power radiation by randomly vibrating pipewalls*, J. Acoust. Soc. Am., 5 (1977).

[7] D. T. LAIRD, H. COHEN, *Directionality patterns for acoustic radiation from a source on a rigid cylinder*, J. Acoust. Soc. Am., 24 (1952).

[8] M. MENŻYŃSKI, *Analysis of the emission of vibroacoustic energy of the reduction lines of gas installations, for its limitation* (in Polish), Doct. diss., Academy of Mining and Metallurgy, 1982.

Received on 7 March, 1983; revised version on 27 April 1984.

ARCHIVES OF ACOUSTICS
9, 4, 305-324 (1984)

Ultra- and hypersonic properties of the critical mixture *n* - amyl alcohol - nitromethane

MIKOŁAJ ŁABOWSKI, TOMASZ HORNOWSKI

Chair of Acoustics, Adam Mickiewicz University
(60-769 Poznań, ul. Matejki 48/49)

This paper gives the results of experimental investigations of the propagation velocity and the absorption coefficient of acoustic waves, both in the ultra - and hypersonic ranges, in the critical mixture *n* - amyl alcohol - nitromethane for two temperatures. The values of α/f^2 obtained experimentally were compared with those resulting from FIXMAN's and CHABAN's theory. It was found that both theories can, with some restrictions, describe experimental results.

1. Introduction

The investigations of the absorption of acoustic waves in a large number of critical mixtures showed that in those mixtures there is an additional range of acoustic dispersion which is not observed in low - viscosity single - component liquids [1-3]. It was shown [4-6] that the quantity α/f^2 depends on frequency, temperature and concentration. On the curve of the dependence of α/f^2 on concentration there is a maximum corresponding to the critical composition of the mixture, whose value increases rapidly as the frequency of acoustic waves decreases. For all concentrations the existing dispersion of the quantity α/f^2 is not accompanied by changes in the acoustic wave propagation velocity on the frequency scale which are measurable by the methods used.

The rapid increase in the absorption of acoustic waves in mixtures in the direct neighbourhood of the critical point, an increase in the intensity of the central component in the fine structure of Rayleigh light scattering and a large decrease in the diffusion coefficient are caused by an increase in the fluctuation of concentration and an increase in its correlation length with decreasing distance from this point.

It is very essential to investigate phase transitions in liquids and their mixtures of various physical nature, since comparison of the results obtained

with the behaviour of pure media provides the possibility of explaining the character of mutual interactions among the different molecules of the liquid. Therefore, of necessity, the gathering of experimental data on the properties of mixtures over a wide range of temperatures, pressures, concentrations and frequencies is now an important cognitive problem.

The present paper gives the results of investigations of acoustic properties over a wide frequency range in a pure component and in the critical mixture *n* - amyl alcohol - nitromethane for different concentrations and two temperatures. The results obtained were compared with those based on formulae resulting from FIXMAN's and CHABAN's respective theories.

The choice of this mixture for the investigations was suggested by lack of information on its acoustic properties over a wide frequency range, and in addition by the purpose of carrying out hypersonic investigations in the neighbourhood of the critical point. This was possible because the refractive indices in individual components are hardly different from each other and due to this, critical opalescence does not occur in the neighbourhood of the critical point.

2. Method of the experiment

The propagation velocity and the absorption coefficient of acoustic waves were measured at two independent measuring stands operating at frequencies of 20 MHz to 150 MHz, by using appropriately the pulse method with resonance excitation of piezoelectric transducers, and at hypersonic frequencies, by taking advantage of the shift and half - width of the Mandelsztam - Brillouin components in the fine structure of the Rayleigh light scattering lines [1, 7]. A detailed description of the measurement equipment, the investigation method and the accuracy of determining the propagation velocity and the absorption coefficient of acoustic waves, both in the ultra - and hypersonic ranges (with photoelectrical registration of the Mandelsztam - Brillouin components) were given in paper [4].

3. Theory

Among the large number of attempts to explain the characteristic behaviour of mixtures close to the critical point, it appeared that the most useful were those which consider the coupling between the concentration fluctuation and the acoustic wave. Far from the critical point, the concentration fluctuation in different volume elements can be regarded as independent. With decreasing distance from the critical point there is a rapid increase in the magnitude of the fluctuations and in their correlation length.

The presence of the acoustic wave in the medium causes a change in the mean amplitude of the concentration fluctuation and in its distribution fun-

ction. The fluctuation distribution reaches a value in equilibrium with some delay, depending on the diffusion coefficient D. The energy of the acoustic wave is used for the change in the fluctuation distribution and then dissipated in the form of heat. This process is irreversible, i.e. it leads to the absorption of acoustic waves. At appropriately high frequencies of the acoustic wave over one period, there is not enough time for a change to occur in the distribution of the concentration fluctuations and no absorption caused by these fluctuations can be observed.

This relaxation model is the basis for both FIXMAN's and CHABAN's theories, which describe the propagation of acoustic waves in mixtures close to their critical point. The two theories differ in the method of calculations and by some additional assumptions.

According to FIXMAN, a change in the fluctuation distribution occurs only under the effect of adiabatic temperature changes caused by the acoustic wave. On this assumption, FIXMAN calculated [8, 9] the additional contribution to the specific heat, related to this process. He also assumed that this process makes the same contribution to the specific heat at constant pressure and at constant volume (in the light of the current investigations, this assumption is not true [10]), and on this assumption he calculated the velocity and the absorption coefficient of the acoustic wave.

From DEBYE's formula [11],

$$\varkappa^2 = (6/l^2 T_c)|T - T_c|, \tag{1}$$

where $\varkappa^{-1} = \xi$ is the correlation length of the concentration fluctuation, l is the radius of intermolecular interractions and T_c is the critical temperature; the final result of FIXMAN's theory can be given in the following from:

$$\frac{a}{f^2} = Af^{-5/4} Im[f(d)] + B, \tag{2}$$

$$v = v_\infty \{1 - Av_\infty f^{-1/4} Re[f(d)]\}, \tag{3}$$

where

$$f(d) = \frac{1}{\sqrt{d}} \int_0^\infty \frac{z^4}{(z^2+1)\,[z^2(z^2+1) - id^{-2}]}\, dz, \qquad z = k\xi, \tag{4}$$

$$d = Cf^{-1/2}|T - T_c|, \tag{5}$$

with v_∞ being the acoustic wave velocity at $\omega\tau \gg 1$. The constants A and C weakly dependent on temperature and independent of frequency.

The function $f(d)$ was defined numerically by KENDIG and others [12].

The analytical form of this function,

$$f(d) = \frac{1}{2}\pi i d^{3/2}\{1-i(1+4id^{-2})^{-1/2}(x_1^{5/2}+x_2^{5/2})\},$$
$$x_1 = -\frac{1}{2}+\frac{1}{2}(1+4id^{-2})^{1/2}, \quad x_2 = -(x_1+1), \tag{6}$$

which will be used in the further part of this paper, was given by FIXMAN.

CHABAN, on the basis of the more recent papers by KAWASAKI [13], KADANOFF and SWIFT [14], modified to some extent FIXMAN's assumptions about the change in the fluctuation distribution under the effect of acoustic waves. This permitted some intrinsic inconsistencies of FIXMAN's theory to be avoided [15].

CHABAN assumed that the change in the fluctuation distribution under the effect of acoustic waves occurs not only as a result of adiabatic temperature changes, but it is also caused by rapid changes in the critical temperature effected by the pressure of the acoustic wave.

On the basis of these assumptions, CHABAN determined the complex adiabatic compressibility of a medium with strong concentration fluctuations [16]. From the fluctuation dissipation theorem, he calculated the change in the fluctuation distribution caused by the acoustic wave. His considerations gave the following final results [17]:

$$v = v_0\left\{1-\frac{Mv_0}{2\pi\tau_1}[|T-T_c|+a|\bar{x}-\bar{x}_c|^3]^{-0,2}\left[F_2(\omega\tau)-\frac{b-\tan^{-1}b}{12}\right)\right\}, \tag{7}$$

$$\frac{\alpha}{f^2} = M[|T-T_c|+a|\bar{x}-\bar{x}_c|^3]^{-2}F_1(\omega\tau)+L, \tag{8}$$

where

$$F_1(\omega\tau) = \int_0^\infty \frac{z^4\frac{3}{4}\left[\frac{1}{z^2}+1+\left(z-\frac{1}{z^3}\right)\tan^{-1}z\right]dz}{\left\{(\omega\tau)^2+4z^4\frac{9}{16}\left[\frac{1}{z^2}+1+\left(z-\frac{1}{z^3}\right)\tan^{-1}z\right]^2\right\}(1+z^2)^2},$$

$$F_2(\omega\tau) = \int_0^\infty \frac{2z^6\frac{9}{16}\left[\frac{1}{z^2}+1+\left(z-\frac{1}{z^3}\right)\tan^{-1}z\right]^2 dz}{\left\{(\omega\tau)^2+4z^4\frac{9}{16}\left[\frac{1}{z^2}+1+\left(z-\frac{1}{z^3}\right)\tan^{-1}z\right]^2\right\}(1+z^2)^2},$$

$$\tau = \frac{\tau_1}{2\pi}[|T-T_c|+a|\bar{x}-\bar{x}_c|^3]^{-1/3}, \tag{9}$$

v_0 is the acoustic wave velocity at $\omega\tau \ll 1$, x_c is the critical concentration of the mixture, M and L are constants weakly dependent on temperature and concentration and independent of frequency. It follows from theoretical calculations that $b \cong 5$. Expressions (7) and (8) are valid with the condition $\omega\tau < 340$ [18].

Both in FIXMAN's and CHABAN's theories, the constants A and C and M and τ are represented by means of the parameters of the mixture, however, it is quite difficult to determine some of them, e.g. the correlation length or the diffusion constant. Therefore, these constants are most frequently determined from the condition of best agreement between theory and experiment. This method was also assumed in the present paper.

The parameters of the curves of the "best fit" were determined by using the least squares method, i.e. by minimizing the expression

$$\chi_\nu^2 = \sum_{j=1}^{n} \frac{[\hat{y}_j - f(x_1 \ldots x_m)]^2}{\sigma_j^2}, \tag{10}$$

where $\hat{y}_j$ is an experimentally determined quantity, n is the number of measurements, m is the number of constants to be determined, σ_j^2 is the squared mean error of the jth measurement and $\nu = n - m$ is the number of degrees of freedom.

The function $Im[f(d)]$ and $F_1(\omega\tau)$, their derivatives and the parameters of the curves of the "best fit" were computed on a Sinclair ZX-81 minicomputer, where the following analytical form of the function $\mathrm{Im}[f(d)]$ was assumed:

$$\mathrm{Im}[f(d)] = \frac{1}{2}\pi d^{3/2}\left[1 + \sqrt{\frac{(\Delta_1)^5}{\Delta}}\sin\left(\frac{5\vartheta_1 - \vartheta}{2}\right) + \sqrt{\frac{(\Delta_2)^5}{\Delta}}\sin\left(\frac{5\vartheta_2 - \vartheta - 2\pi}{2}\right)\right], \tag{11}$$

where

$$\Delta = \frac{1}{d^2}\sqrt{d^4+16}, \quad \vartheta = \tan^{-1}\frac{4}{d^2},$$

$$\Delta_1 = \left(\frac{1}{4} + \frac{1}{4}\Delta - \frac{1}{2}\sqrt{\Delta}\cos\frac{\vartheta}{2}\right)^{1/2}, \quad \Delta_2 = \left(\frac{1}{4} + \frac{1}{4}\Delta + \frac{1}{2}\sqrt{\Delta}\cos\frac{\vartheta}{2}\right)^{1/2},$$

$$\vartheta_1 = \tan^{-1}\left(\frac{\sin\frac{\vartheta}{2}}{\cos\frac{\vartheta}{2} - \frac{1}{\sqrt{\Delta}}}\right), \quad \vartheta_2 = \tan^{-1}\left(\frac{\sin\frac{\vartheta}{2}}{\cos\frac{\vartheta}{2} + \frac{1}{\sqrt{\Delta}}}\right) + \pi.$$

The values of the function $F_1(\omega\tau)$ were calculated by means of the Simpson quadrature, by transformation of the variables $x = \tan\alpha$.

$$F_1(\omega\tau) = \frac{3}{8}\int_0^{\pi/2} \frac{(\sin 2\alpha)^3 g(\alpha)\, d\alpha}{4(\omega\tau)^2 \cos^6\alpha \sin^2\alpha - 9g^2(\alpha)},$$

$$g(\alpha) = \frac{1}{2}\sin 2\alpha - \alpha\cos 2\alpha.$$

The derivatives of the functions $Im[f(d)]$ and $F_1(\omega\tau)$ were approximated by the difference quotient

$$F' \cong \frac{f(x_0+\delta x) - f(x_0)}{\delta x}.$$

Since both in CHABAN's and FIXMAN's theories there are nonlinear dependencies, therefore the fitting process must be carried out by successive approximations. This process should be stopped when the value of χ^2 reaches a minimum with the predescribed magnitude of the measurement error.

4. Investigation results and discussion

a) Ultra and hypersonic properties of pure nitromethane

Measurements over the frequency range 29-130 MHz showed that within the measurement error α/f^2 does not depend on frequency. At a frequency of about 4.1 GHz the value of α/f^2 decreases, and there is also a slight increase in the acoustic wave propagation velocity.

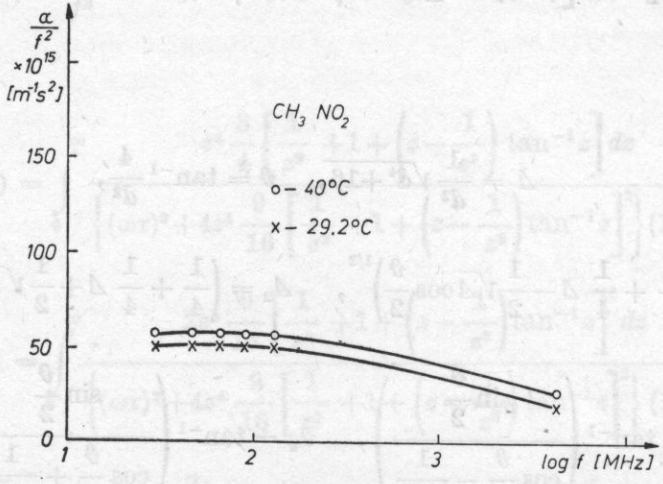

Fig. 1. The dependence of α/f^2 on $\log f$ in nitromethane for temperatures of 29.2°C and 40°C

The results of measurements of the quantity α/f^2 in pure nitromethane over the whole range of the frequencies investigated for two temperatures are shown graphically in Fig. 1. This figure indicates a slight increase in α/f^2 as temperature increases.

By using the formula

$$\tau = \frac{1}{\omega_n}\left[\left(\frac{\alpha'}{f^2}\right)_{f\to 0}\Big/\left(\frac{\alpha'}{f^2}\right)_{f=f_n} - 1\right]^{1/2}, \tag{12}$$

the acoustic relaxation time τ was estimated to be about $0.7\cdot 10^{-10}$s.

Subsequently, using the estimated value of the relaxation time τ, the value of the propagation velocity of hypersonic waves was determined at a frequency of about 4100 MHz for $T = 29.2°C$, from the following relation:

$$\frac{v_0^2}{v^2} = 1 - \varepsilon\frac{\omega^2\tau^2}{1+(\omega\tau)^2}, \tag{13}$$

where

$$\varepsilon = \frac{A' v_0}{2\pi\tau}.$$

The experimental value of the propagation velocity of hypersonic waves for this temperature is 1350 m/s, while the one estimated according to the above method is about 1362 m/s. The above values of the velocity of hypersonic waves within the experimental error are sufficiently close to permit the relaxation process in nitromethane to be characterized by one relaxation time.

The respective values of some physical - chemical and acoustic quantities are given in Table 1. It follows from this table that the values of c^*_{opt} and c^*_{ac} coincide within the experimental error. The values of c^*_{opt} are found from data on the normal frequencies of the molecule vibration by means of the Planck - Einstein formula [1].

An increase in a_{ex}/f^2 and in the ratio η_v/η_s with increasing temperature indicates that there is oscillation relaxation. The investigations in [19] showed that in pure *n* - amyl alcohol there is structural relaxation. It can be expected that when in the mixture *n* - amyl alcohol - nitromethane acoustic dispersion is observed at frequencies lower than about 10^9 Hz, it will be caused by the relaxation of the concentration fluctuation.

b) Ultra - and hypersonic properties of the critical mixture n - amyl alcohol - nitromethane

The mixture *n* - amyl alcohol - nitromethane has an upper critical point. The critical parameters determined are respectively: $T_c = 27.8°C$ and $x_c = 0.385$ (x_c - molar fraction of *n* - amyl alcohol). The critical temperature was determined visually from the vanishing boundary between phases and from the maximum intensity of the central component of scattered light.

Table 1

T [°C]	$A \cdot 10^{15}$ [$m^{-1}s^2$]	$\frac{\alpha_{cl}}{f^2} \cdot 10^{15}$ [$m^{-1}s^2$]	$\frac{\alpha_{exp}}{\alpha_{cl}}$	$\frac{\eta_v}{\eta_s}$	$\tau \cdot 10^{10}$ [s]	v_0 [m/s]	v_h [m/s]	$\Delta\nu$ [cm^{-1}]	c_p $\left[\frac{cal}{moldeg}\right]$	c_v $\left[\frac{cal}{moldeg}\right]$	c^*_{opt} $\left[\frac{cal}{moldeg}\right]$	c^*_{ac} $\left[\frac{cal}{moldeg}\right]$
29.2	39	6.5	8.2	9.4	0.7	1305	1350	0.15	24.6	16.2	4.8	4.2
40	40	6.3	8.9	10.6	0.8	1260	1296	0.13	—	—	—	—

Table 2

$n-C_5H_{11}OH$ in CH_3NO_2	$\Delta\nu$ [cm^{-1}]	f_h [GHz]	v_0 [m/s]	v_h [m/s]	$\frac{I_c}{2I_{MB}}$	$\alpha/f^2 \cdot 10^{15}$ [s^2/m]	$\Delta\nu_{MB} \cdot 10^3$ [cm^{-1}]	ϱ [kg/m^3]
0.0	0.141	4.23	1340	1374	0.6	19.15	5	1124.1
0.1	0.132	3.96	1270	1285	0.7	28.04	6	1079.0
0.3	0.130	3.90	1248	1257	6.4	73.89	15	972.4
0.385	0.128	3.84	1232	1237	17.8	82.62	16	958.2
0.5	0.133	3.99	1240	1281	7.2	64.66	14	927.6
0.9	0.132	3.96	1243	1264	0.5	47.50	10	839.6
1.0	0.130	3.90	—	1237	0.3	20.02	4	814.8

Fig. 2 shows the dependence of the temperature of the separation of the components of the mixture for different concentrations.

Fig. 3. shows the results of measurements of the light refractive index on concentration in the mixture n - amyl alcohol - nitromethane at a temperature of 29.2°C.

The measurements showed that n changes depending on composition in a rather linear way and does not "feel" the critical point. The light refractive indices of pure components of this mixture at 29.2°C differ slightly, therefore in practice, hardly any critical opalescence occurs in it, which permits the observation of the fine structure of the Rayleigh light scattering also in the direct neighbourhood of the temperature of the separation of the components.

In the experiment, chemically pure media were used, which were additionally cleaned chemically and distilled several times. The degree of purity was controlled by measuring the refractive index density and the boiling temperature. The cell filled with the mixture was sealed by welding so as to decrease the volume of the gas phase and to maintain the constant composition of the mixture in the course of optical measurements.

In order to gain essential information about the kinetics of the concentration fluctuation, acoustic investigations of the properties of the mixture n - amyl

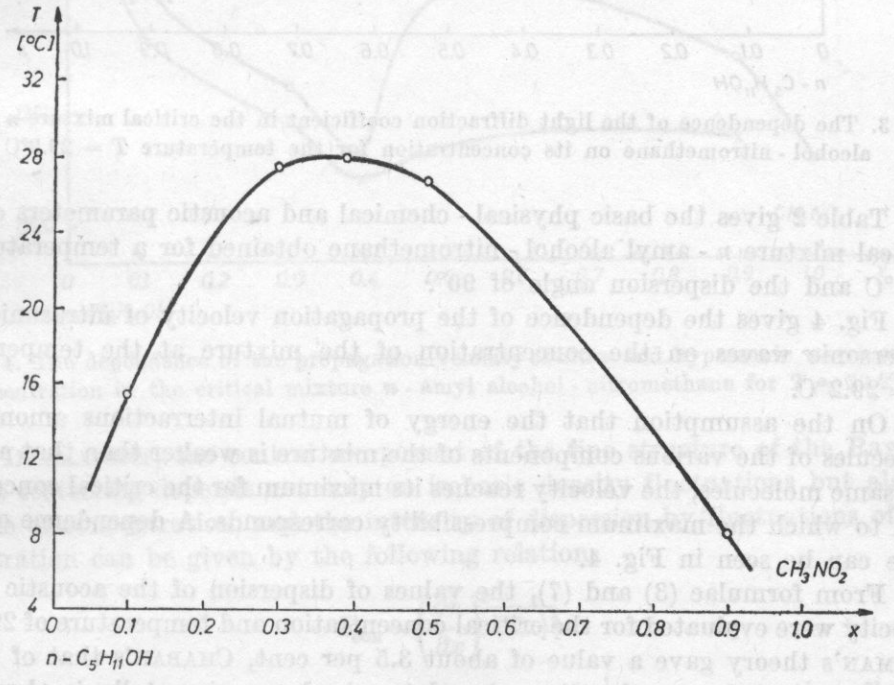

Fig. 2. The curve of the separation of the components of the system n - amyl alcohol-nitromethane. The concentration of the components expressed in molar fraction

alcohol - nitromethane were carried out for the following concentrations: $x = 0.1, 0.3, 0.385, 0.5, 0.9$ molar fraction of n - amyl alcohol.

The acoustic wave propagation velocity was determined for two frequencies: 28 HMz and about 3900 MHz. The amplitude coefficient of the absorption of acoustic waves was determined over the ultrasonic range 29.6-128.6 MHz by the pulse method, using the resonance excitation of piezoelectric transducers, and over the hypersonic range the fine structure of the Rayleigh light scattering.

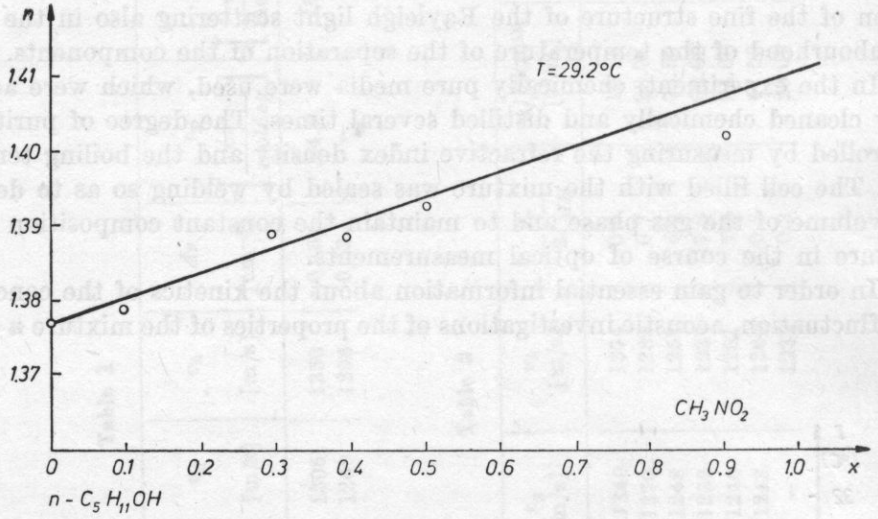

Fig. 3. The dependence of the light diffraction coefficient in the critical mixture n - amyl alcohol - nitromethane on its concentration for the temperature $T = 29.2°C$

Table 2 gives the basic physical - chemical and acoustic parameters of the critical mixture n - amyl alcohol - nitromethane obtained for a temperature of 29.2°C and the dispersion angle of 90°.

Fig. 4 gives the dependence of the propagation velocity of ultrasonic and hypersonic waves on the concentration of the mixture at the temperature $T = 29.2°C$.

On the assumption that the energy of mutual interractions among the molecules of the various components of the mixture is weaker than that among the same molecules, the velocity reaches its maximum for the critical concentration to which the maximum compressibility corresponds. A dependence of this type can be seen in Fig. 4.

From formulae (3) and (7), the values of dispersion of the acoustic wave velocity were evaluated for the critical concentration and temperature of 29.2°C. FIXMAN's theory gave a value of about 3.5 per cent, CHABAN's that of about 0.6 per cent, whereas the dispersion determined experimentally is about 0.4 per cent.

As was already mentioned, in pure nitromethane and n - amyl alcohol, over the frequency range 29.6-128.6 MHz, the quantity α/f^2 does not depend on frequency within the experimental error, and for hypersonic frequencies a deviation from the Stokes law can be observed.

The present paper demonstrates that the relaxation process in pure nitromethane is caused by the oscillation relaxation, while it was proved in paper [19] that the structural relaxation is responsible for the relaxation process in n - amyl alcohol.

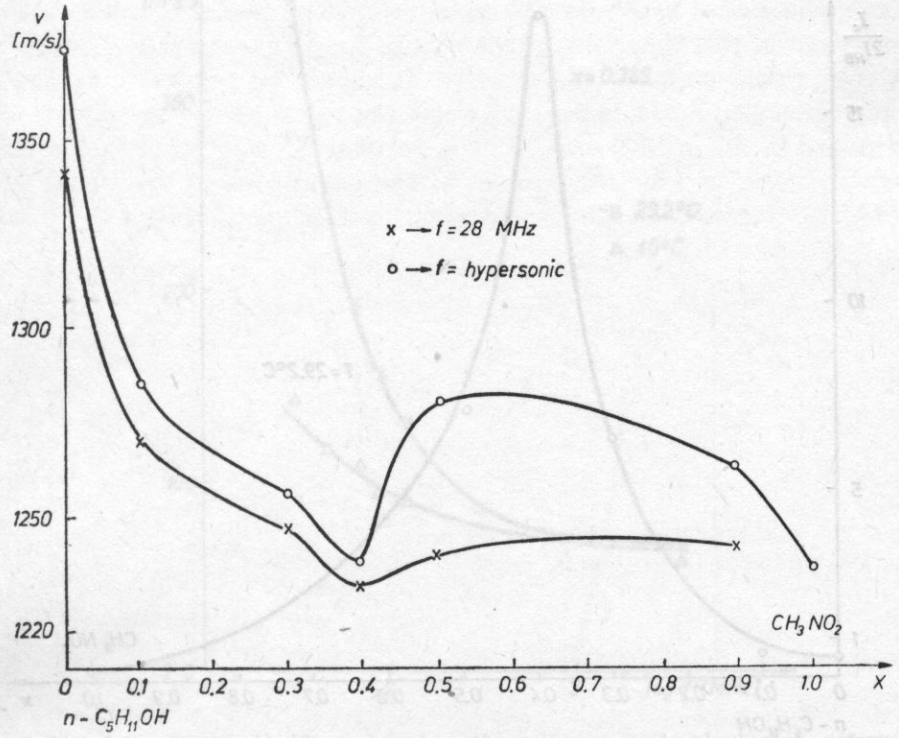

Fig. 4. The dependence of the propagation velocity of ultra- and hypersonic waves on concentration in the critical mixture n - amyl alcohol - nitromethane for $T = 29.2°C$

In mixtures, the central component of the fine structure of the Rayleigh light scattering depends not only on isobaric density fluctuations but also on those of concentration, and the intensity of dispersion by fluctuations of concentration can be given by the following relation:

$$I_{\text{con}} \sim \left(\frac{\partial n}{\partial x}\right)^2 \overline{(\Delta x)^2}.$$

In the mixture n - amyl alcohol - nitromethane, concentration fluctuations can be observed, which increase as the temperature and concentration

approach their values at the critical point. Therefore, $I_c/2I_{MB}$ reaches for this mixture its maximum values close to the critical parameters, which can be seen in Fig. 5, where the dependence of $I_c/2I_{MB}$ on the composition of the mixture is given for the temperature $T = 29.2°C$.

A considerable increase in the value of the ratio $I_c/2I_{MB}$ as the mixture approaches the critical parameters indicates strong light scattering by concentration fluctuations and by isobaric density fluctuations, with the simultaneous decrease in the effect of adiabatic density fluctuations.

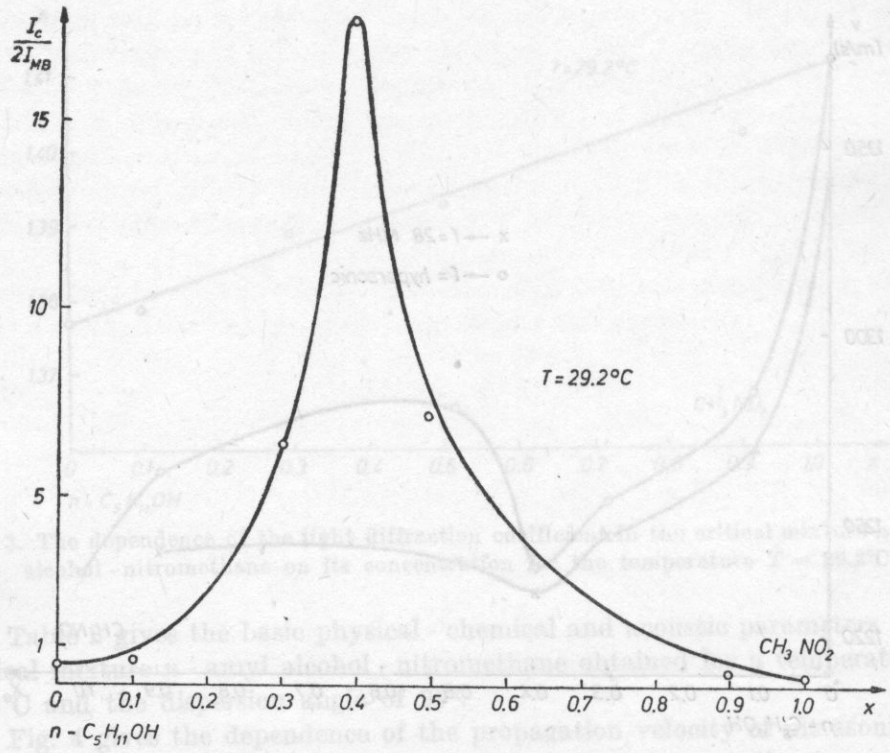

Fig. 5. The dependence of $I_c/2I_{MB}$ on concentration in the critical mixture n - amyl alcohol - nitromethane at the temperature $T = 29.2°C$ (x - molar fraction of n - amyl alcohol)

In the mixture n - amyl alcohol - nitromethane considerable depolarised spectrum can be observed, which reaches its maximum values in the direct neighbourhood of the critical point, indicating that it is possible to observe and measure the scattering by the orientation fluctuations.

Experimental points representing the dependence of α/f^2 on frequency are plotted in Figs. 6-8 respectively for three concentrations and two temperatures. The solid lines in these figures were plotted on the basis of formulae (2) and (5) resulting from FIXMAN's theory.

The values of the parameters of the "best fit curves" are listed in Table 3.

In Figs. 9-11 the solid curves were plotted from formulae (8) and (9), resulting from CHABAN's theory.

On the basis of this theory, the following values of the parameters of the curves of the "best fit" were obtained: $M = 2.751 \cdot 10^{-11} s^2 deg^2 m^{-1}$, $\tau_1 = 2.166 \cdot 10^{-7} s$, $L = 60.1 \cdot 10^{-15} s^2 m^{-1}$.

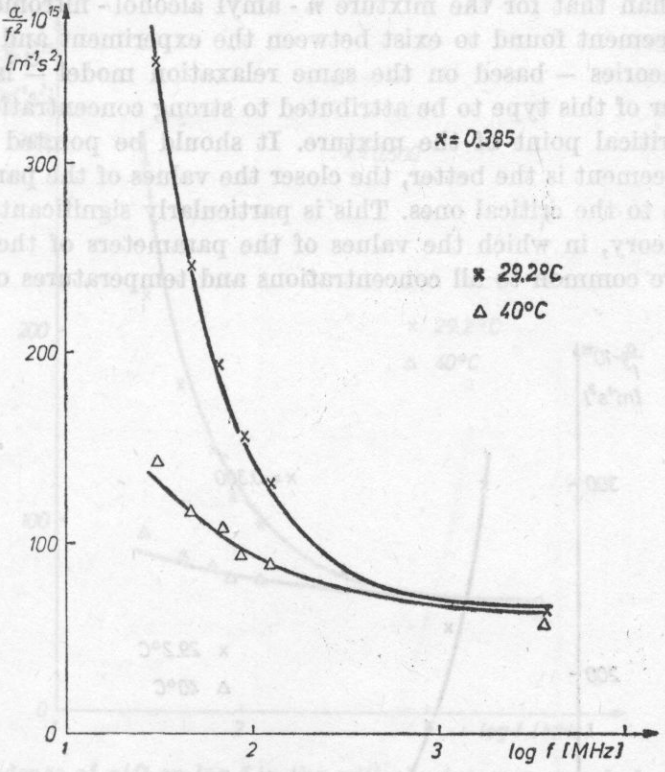

Fig. 6. The dependence of α/f^2 on log f in the mixture n - amyl alcohol - nitromethane with the critical concentration $x = 0.385$ (x - molar fraction of n - amyl alcohol) for two temperatures. The solid curves were plotted from formulae (2) and (5). x, Δ - experimental points

The quantity a in equation (9) was determined from the dependence of the separation temperature of the mixture on concentration. It is $a = 400$ deg/ /molar fraction.

Figs. 12 and 13 give the dependence of the quantity α/f^2 on concentration for different frequencies for the mixture n - amyl alcohol - nitromethane.

Figs. 12 and 13 indicate that in the mixture n - amyl alcohol - nitromethane the quantity α/f^2 passes a maximum at $x_c = 0.385$. The value of this maximum

decreases as the frequency increases, and it almost vanishes at hypersonic frequencies.

This effect cannot be explained by an increase in the shear viscosity, which increases slightly only in the direct neighbourhood of the critical point [20], or by relaxation processes occurring in the pure components of the mixture. It was shown experimentally that in the pure components of the mixture the quantity α/f^2 hardly depends on frequency and is lower by several orders of magnitude than that for the mixture n - amyl alcohol - nitromethane.

The agreement found to exist between the experiment and FIXMAN's and CHABAN's theories — based on the same relaxation model — is the basis for the behaviour of this type to be attributed to strong concentration fluctuations about the critical point of the mixture. It should be pointed out, however, that this agreement is the better, the closer the values of the parameters of the mixtures are to the critical ones. This is particularly significant in the case of CHABAN's theory, in which the values of the parameters of the curves of the "best fit" are common to all concentrations and temperatures of the mixture,

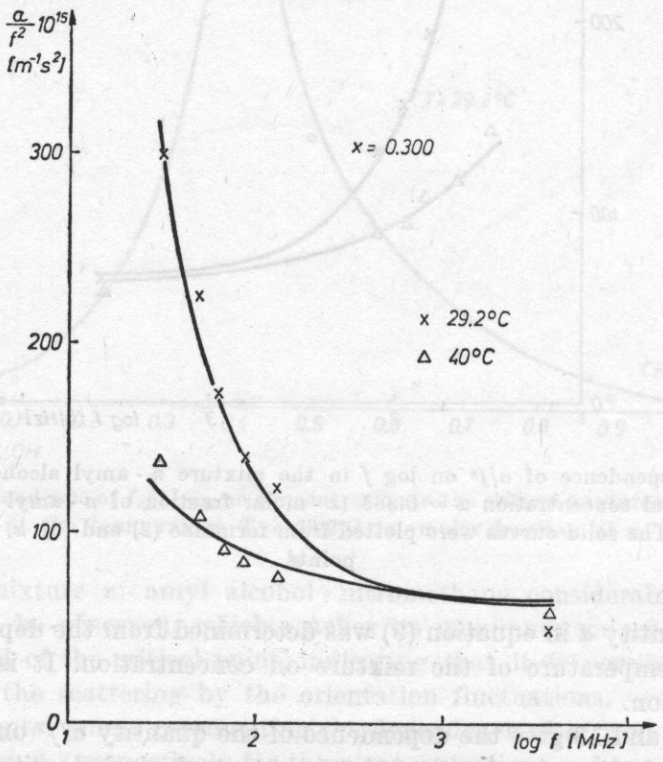

Fig. 7. The dependence of α/f^2 on $\log f$ in the critical mixture n - amyl alcohol - nitromethane with the concentration $x = 0.300$ (x - molar fraction of n - amyl alcohol) for two temperatures. The solid curves were plotted from formulae (2) and (5). x, Δ - experimental points

in contrast to FIXMAN's theory, where the constants A and C, dependent on concentration, must be selected for each concentration.

The attempts to generalize FIXMAN's theory [6, 21], i.e. a description of the absorption coefficient as function of concentration, based on the Flory-Huggins approximation, give very poor agreement between theory and experiment (with maxima usually displaced towards higher concentrations, and the simultaneous decrease in their value).

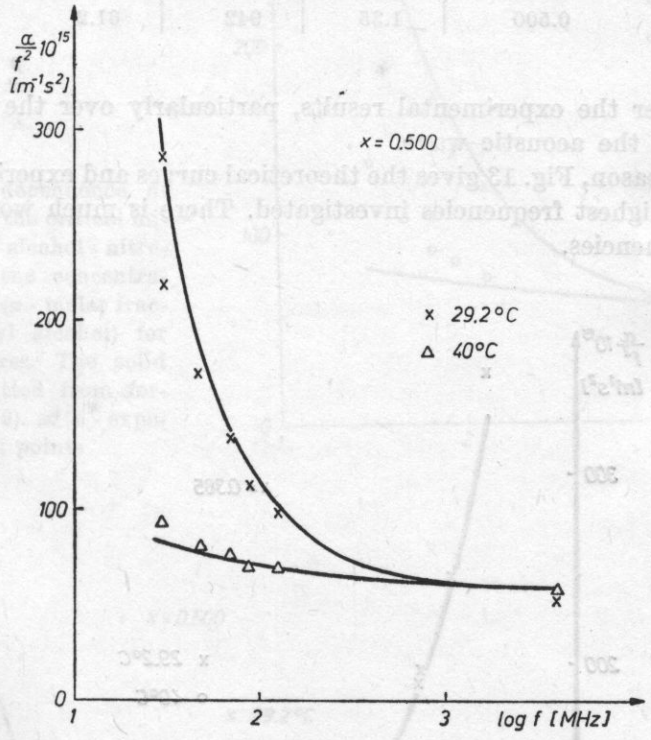

Fig. 8. The dependence of α/f^2 on log f in the critical mixture n - amyl alcohol - nitromethane with the concentration $x = 0.500$ (x - molar fraction of n - amyl alcohol) for two temperatures. The solid curves were obtained from formulae (2) and (5). x, Δ - experimental points

Neglecting the Flory - Huggins approximation would require that the additional quantity $(\partial\mu/\partial x)_{p,T}$ should be determined from the total intensity of the central component of the scattered light.

At the present stage of investigations, CHABAN's theory is more convenient than FIXMAN's, as it permits - while requiring determination of a smaller number of parameters - the acoustic parameters of critical mixtures to be described with greater complexity.

In the case of the mixture n - amyl alcohol - nitromethane, the dependence of the quantity α/f^2 on concentration, determined from CHABAN's theory,

Table 3

Concentration in molar fractions of n-amyl alcohol	$A \cdot 10^3$ [$s^{3/4}m^{-1}$]	C [$s^{-1/2}deg^{-1}$]	$B \cdot 10^{15}$ [$m^{-1}s^2$]
0.385	2.07	574	66.6
0.300	1.72	567	65
0.500	1.35	942	61.2

describes better the experimental results, particularly over the higher frequency range of the acoustic wave.

For this reason, Fig. 13 gives the theoretical curves and experimental results only for the highest frequencies investigated. There is much worse agreement at lower frequencies.

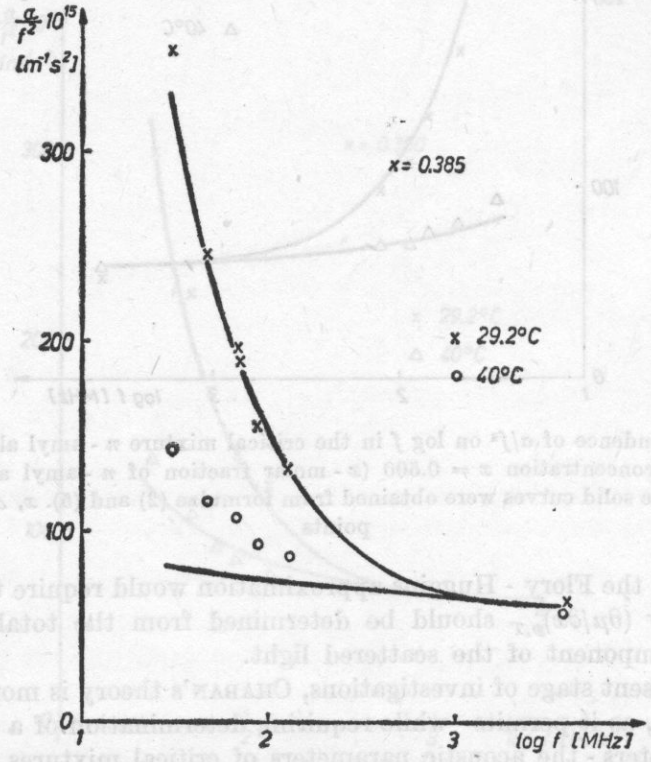

Fig. 9. The dependence of α/f^2 on log f in the mixture n - amyl alcohol - nitromethane with the critical concentration $x = 0.385$ (x - molar fraction of n - amyl alcohol) for two temperatures. The solid curves were plotted from formulae (8) and (9). x, o - experimental points

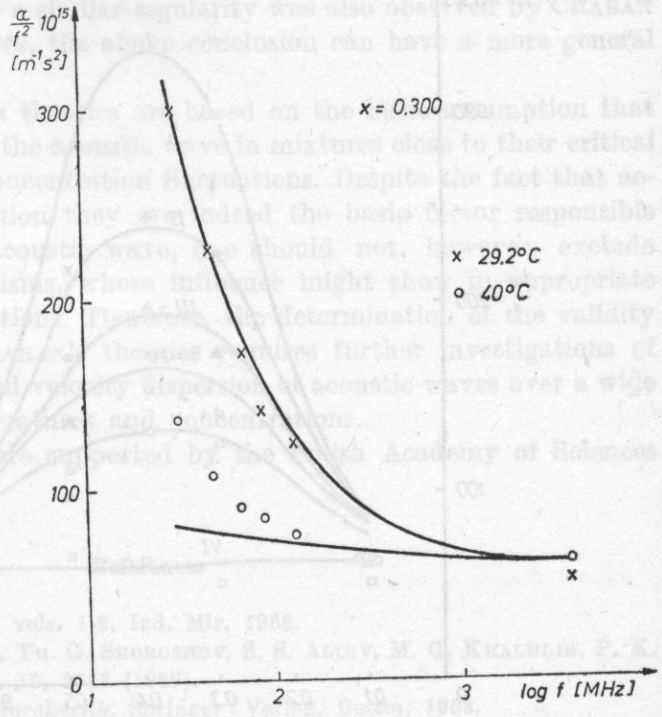

Fig. 10. The dependence of α/f^2 on log f in the critical mixture n - amyl alcohol - nitromethane with the concentration $x = 0.300$ (x - molar fraction of n - amyl alcohol) for two temperatures. The solid curves were plotted from formulae (8) and (9). x, o - experimental points

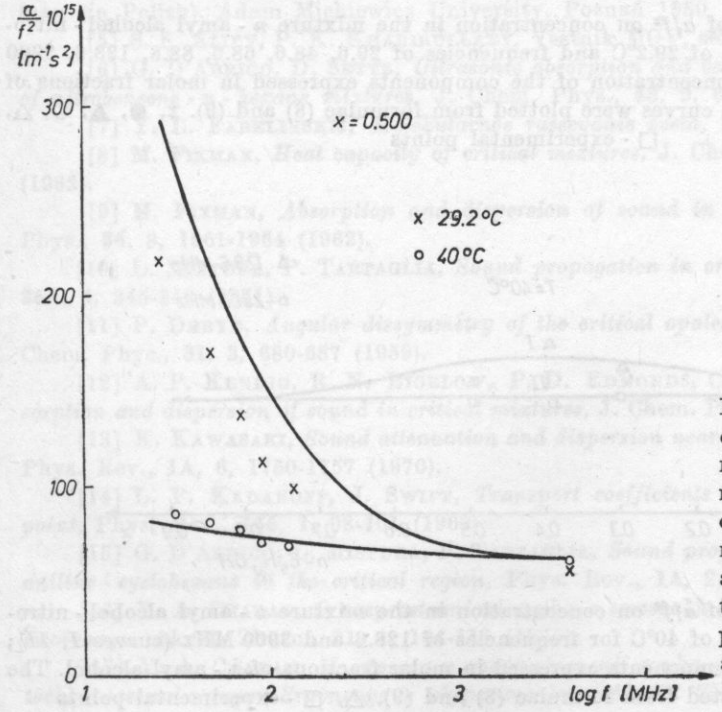

Fig. 11. The dependence of α/f^2 on log f in the critical mixture n - amyl alcohol - nitromethane with the concentration $x = 0.500$ (x - molar fraction of n - amyl alcohol) for two temperatures. The solid curves were plotted from formulae (8) and (9). x, o - experimental points

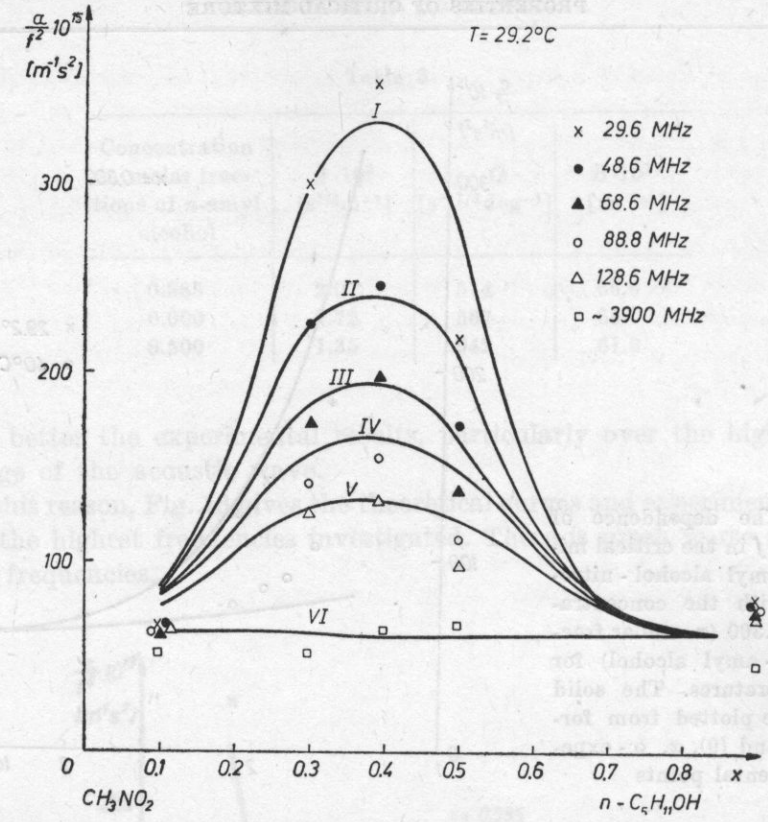

Fig. 12. The dependence of α/f^2 on concentration in the mixture *n* - amyl alcohol - nitromethane at a temperature of 29.2°C and frequencies of 29.6, 48.6, 68.6, 88.8, 128.6, 3900 MHz (curves I-VI); the concentration of the components expressed in molar fractions of *n* - amyl alcohol. The solid curves were plotted from formulae (8) and (9). x, ●, ▲, ○, △, □ - experimental points

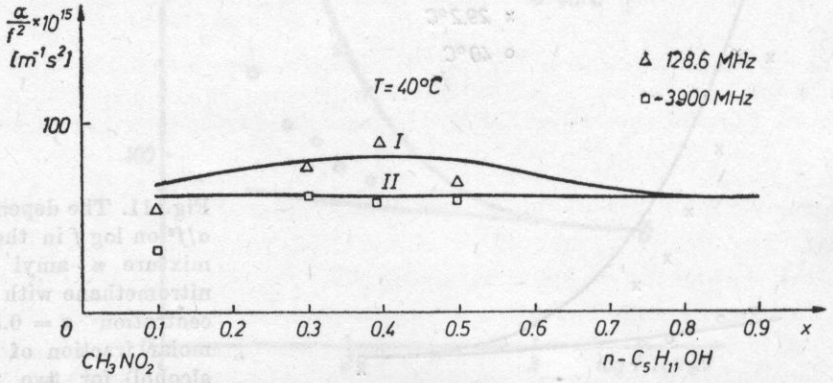

Fig. 13. The dependence of α/f^2 on concentration in the mixture *n* - amyl alcohol - nitromethane at a temperature of 40°C for frequencies of 128.6 and 3900 MHz (curves *I*, *II*); the concentration of the components expressed in molar fractions of *n* - amyl alcohol. The solid curves were plotted from formulae (8) and (9). △, □ - experimental points

In view of the fact that a similar regularity was also observed by CHABAN [17] in other critical mixtures, the above conclusion can have a more general nature.

FIXMAN's and CHABAN's theories are based on the basic assumption that the anomalous behaviour of the acoustic wave in mixtures close to their critical point is caused by strong concentration fluctuations. Despite the fact that according to the current opinion they are indeed the basic factor responsible for this behaviour of the acoustic wave, one should not, however, exclude the effect of other mechanisms, whose influence might show in appropriate mixtures under some conditions. Therefore, the determination of the validity range of FIXMAN's and CHABAN's theories requires further investigations of the absorption coefficient and velocity dispersion of acoustic waves over a wide range of frequencies, temperatures and concentrations.

These investigations were supported by the Polish Academy of Sciences (Problem MR. I. 24).

References

[1] *Fizicheskaya akustika*, vols. 1-2, Izd. Mir, 1968.

[2] M. Y. SHAKHPARONOV, Yu. G. SHOROSHOV, S. S. ALIEV, M. G. KHALULIN, P. K. KHABIBULLAEV, Zh. F. Ch., **43**, 10, 2543 (1969).

[3] W. SCHAAFFS, *Molekularakustik*, Springer - Verlag, Berlin, 1963.

[4] M. ŁABOWSKI, *Ultra - and hypersonic properties of chosen liquids and critical mixtures* (in Polish), Adam Mickiewicz University, Poznań 1980.

[5] S. S. ALIEV, P. K. KHABIBULLAEV, Vestnik MGV, series Chemiya, 6, 115 (1969).

[6] G. D'ARRIGO, D. SETTE, *Ultrasonic absorption and velocity near the critical region of nitrobenzene - n - hexane mixtures*, J. Chem. Phys., **48**, 2. 691-698 (1968).

[7] Y. L. FABELINSKIJ, *Molekularnoe rasseyanie sveta*, Izd. Nauka, Moscow, 1965.

[8] M. FIXMAN, *Heat capacity of critical mixtures*, J. Chem. Phys., **36**, 8, 1957-1960 (1962).

[9] M. FIXMAN, *Absorption and dispersion of sound in critical mixtures*, J. Chem. Phys., **36**, 8, 1961-1964 (1962).

[10] L. MIXTURA, P. TARTAGLIA, *Sound propagation in critical mixtures*, Phys. Lett., **36A**, 4, 345-348 (1971).

[11] P. DEBYE, *Angular dissymmetry of the critical opalescence in liquid mixtures*, J. Chem. Phys., **31**, 3, 680-687 (1959).

[12] A. P. KENDIG, R. N. BIGELOW, P. D. EDMONDS, C. J. PINGS, *Comment on absorption and dispersion of sound in critical mixtures*, J. Chem. Phys., **40**, 5, 1451 (1964).

[13] K. KAWASAKI, *Sound attenuation and dispersion near the liquid - gas critical point*, Phys. Rev., **1A**, 6, 1750-1757 (1970).

[14] L. P. KADANOFF, J. SWIFT, *Transport coefficients near the liquid - gas critical point*, Phys. Rev., **166**, 1, 98-101 (1968).

[15] G. D'ARRIGO, L. MISTURA, P. TARTAGLIA, *Sound propagation in the binary system aniline - cyclohexane in the critical region*, Phys. Rev., **1A**, 2, 286-296 (1970).

[16] Y. A. CHABAN, *O rasprostranieni zvuka v smesyakh vblizi kriticheskoy tochki rasswaivanya*, Akust. Zhurn., **21**, 1, 104-111 (1975).

[17] Y. A. CHABAN, *K voprosu o rasprostranenii zvuka v smesyakh vblizi kriticheskoy tochki rasswalavanya. Sravnenye s eksperimentom*, Akust. Zhurn., **21**,2, 286-293 (1975).

[18] Y. A. CHABAN, *Obshchaya teoriya rasprostraneniya zvuka i rasseyaniya sveta v rastvorakh s silnymi fluktuatsiyami kontsentratsi*, *Akust.* Zhurn., **29**, 5, 685-692 (1983).

[19] P. K. KHABIBULLAEV, K. PARPIEV, S. S. ALIEV, L. E. KVASOVA, L. V. WANSHYNA, Vestnik MGU, series Chemiya, 1971.

[20] V. K. SENENCHENKO, Ye. W. ZORINA, Zh. F. Ch., **26**, 520 (1952).

[21] K. RAVINDRA PRASAD, K. C. REDDY, *Ultrasonic studies in the critical system benzyl - alcohol + iso - octane*, Acustica, **53**, 1, 55-58 (1983).

Received on 13 December, 1983.

ARCHIVES OF ACOUSTICS
9, 4, 325-339 (1984)

PROBLEM OF THE INSTANTANEOUS SOUND FREQUENCY MEASUREMENT

EDWARD OZIMEK, LECH JUGOWAR, LEON RUTKOWSKI

Institute of Acoustics, Adam Mickiewicz University
(60-769 Poznań, ul. Matejki 48/49)

This paper presents a method for the measurement of the so - called quasi-instantaneous frequency of acoustic signals, which is an approximation of the instantaneous frequency defined on the basis of theoretical considerations. It also describes a measurement system of the (T, f-V) type which was built for this purpose, at the output of which the instantaneous value of the voltage V is proportional to the value of the quasi - period T_q or the quasi - instantaneous frequency f_q of a signal fed to the input. This system permits continuous registration of variations of the quasi - instantaneous frequency in real time. The characteristics of the system (T, f-V) given here and also the oscillograms of chosen test signals (with prescribed modulating functions) and real signals (e.g. those occurring in rooms) indicate the wide possibilities of its use in practice.

1. Introduction

A characteristic feature of most acoustic signals is instantaneous variations in the value of their physical parameters. These variations, which most frequently have the character of irregular fluctuations in amplitude, frequency and phase, carry fundamental information about the signal, which is important e.g. from the point of view of the formation of sound sensation. This is confirmed by the increasingly often carried out psychoacoustic investigations of these variations, based on the so - called dynamic perception, which is understood to be the perception of signals with parameters variable in time. In the range of both these investigations and also some physical research, an essential question is that of the measurement of the signal frequencies rapidly varying in time, which is characterized by its instantaneous frequency. A typical example of such signals are those frequency - modulated, for which the classically conceived frequency is not unambiguous.

In view of this, investigations were undertaken with the basic purpose of developing a conception of the measurement of this frequency rapidly variable in time and designing and constructing an appropriate system to serve for the determination of its instantaneous values.

2. Determination of the instantaneous frequency of a signal

In order to define the notion of the instantaneous frequency, the analytical signal $\Psi(t)$ can be represented in the following exponential form:

$$\Psi(t) = s(t) + j\sigma(t) = \exp[\Phi(t)] = \exp[\mathrm{Re}\,\Phi(t) + j\,\mathrm{Im}\,\Phi(t)], \tag{1}$$

where $\Psi(t)$ is a complex function whose real part is the real signal $s(t) = \mathrm{Re}\{\Psi(t)\}$, while its imaginary part $\sigma(t) = \mathrm{Im}\{\Psi(t)\}$ is the Hilbert transform of the real signal. The modulus of the analytical signal $\Psi(t)$

$$|\Psi(t)| = \sqrt{s^2(t) + \sigma^2(t)} \tag{2}$$

represents the instantaneous amplitude, which will be designated below as $A(t) = |\Psi(t)|$. The instantaneous phase of this signal is defined by the expression

$$\varphi(t) = \tan^{-1}\frac{\sigma(t)}{s(t)}. \tag{3}$$

In turn the complex instantaneous frequency is defined as the quantity $p(t)$, i.e.

$$p(t) = \alpha(t) + j\omega(t) = \frac{d}{dt}\Phi(t) = \frac{d}{dt}\ln\Psi(t) = \frac{1}{\Psi}\frac{d\Psi}{dt}. \tag{4}$$

The following formulation of the analytical signal

$$\Psi(t) = A(t)\exp[j\varphi(t)]$$

and the use of (4) give

$$p(t) = \frac{1}{A(t)\exp[j\varphi(t)]}\frac{d}{dt}[A(t)\exp[j\varphi(t)] = \frac{1}{A(t)}\frac{dA(t)}{dt} + j\frac{d\varphi(t)}{dt}. \tag{5}$$

The real part $\alpha(t)$ of the complex instantaneous frequency $p(t)$ represents in a physical sense a relative increase in the instantaneous amplitude per unit time:

$$\alpha(t) = \frac{1}{A(t)}\frac{dA(t)}{dt}, \tag{6}$$

whereas the imaginary part of $p(t)$ has the meaning of angular frequency,

$$\omega(t) = \frac{d\varphi(t)}{dt}. \tag{7}$$

Using the definition of the complex instantaneous frequency, the analytical signal with the initial amplitude A_0 and the initial phase φ_0 can be given in the form

$$\Psi(t) = A_0 \exp(j\varphi_0) \exp\left[\int_0^t p(t)\,dt\right] = A_0 \exp\left[\int_0^t a(t)\,dt\right] \exp\left[j\left(\int_0^t \omega(t)\,dt + \varphi_0\right)\right]$$

$$= A(t) \exp[j\varphi(t)], \tag{8}$$

where

$$A(t) = A_0 \exp\left[\int_0^t a(t)\,dt\right]$$

represents the instantaneous amplitude of the signal. At the initial time $t = 0$, $A(0) = A_0$. In turn

$$\varphi(t) = \operatorname{Im} \Phi(t) = \int_0^t \omega(t)\,dt + \varphi_0 \tag{9}$$

is the instantaneous phase of the signal. At the initial time $t = 0$, $\varphi(0) = \operatorname{Im} \Phi(0) = \varphi_0$.

In a particular case of a signal with an amplitude constant in time, i.e. for $A(t) = A_0$ and the frequency ω_0, which signifies that $\varphi(t) = \omega_0 t + \varphi_0$, we obtain

$$a(t) = \frac{1}{A(t)} \frac{dA(t)}{dt} = 0$$

and

$$\omega(t) = \frac{d}{dt}(\omega_0 t + \varphi_0) = \omega_0.$$

It can be seen, on the assumption that the instantaneous amplitude of the signal considered is approximately constant or varies relatively slowly with respect to the instantaneous phase of the signal, that the instantaneous frequency is defined by the real quantity $\omega(t)$:

$$\omega(t) = \operatorname{Im} p(t) = \frac{d\varphi(t)}{dt} \tag{10}$$

or, otherwise,

$$f(t) = \frac{1}{2\pi} \frac{d\varphi(t)}{dt}. \tag{10a}$$

It is interesting to note that in the literature [3] one may also find another definition of the instantaneous frequency, based on analysis of the number of zero crossings of the real signal investigated. In this case the instantaneous frequency is defined as the ratio of the number of zero crossings of this signal, determined over some time interval $\Delta\tau$, and the value of this interval. This ratio corresponds to the mean density of zeroes of the signal over this interval and is sometimes called the Rice frequency (f_R):

$$f_R = \lim_{T\to\infty} \frac{N}{\Delta\tau},$$

where N is the number of "positive" or "negative" zero level crossings of the signal and $\Delta\tau$ is the averaging time interval.

It should be pointed out that, depending on the width of the interval $\Delta\tau$ selected, this ratio expresses the mean frequency in this interval, and thus it does not correspond to the strict definition of the instantaneous frequency $\omega(t)$ subordinated to a given time t. E. g. for a frequency - modulated signal, even on the assumption that the interval $\Delta\tau$ is small compared with the period of the modulating frequency, the quantity $\omega(t)$ determined is nevertheless a considerable averaging of the instantaneous frequency, as it occurs for a number of periods of the carrier frequency.

The quantity $\omega(t)$ as defined by expression (10) is thus a theoretical one, as it determines the value of the instantaneous frequency at a given time t, which cannot be implemented in experimental conditions. In these conditions, in expression (10) the differential quantities should be replaced by the difference ones, i.e.

$$\omega(\Delta t) = \frac{\Delta\varphi}{\Delta t}. \tag{11}$$

In keeping with expression (11), the measure of the instantaneous frequency of the signal is the ratio of its phase changes $\Delta\varphi$, occurring over the time interval Δt, and the value of this interval. In experimental terms it is quite intricate to determine phase changes over a very short time interval Δt. Therefore, in the range of the investigations carried out, using the $(T, f-V)$ type system built (see Section 2), measurements were performed of such a time interval $\Delta t = T_q$ in which the signal phase varied by a value of 2π. On this basis, the quantity $\omega(T_q)$ was obtained, equal to

$$\omega(T_q) = \frac{2\pi}{T_q} = 2\pi f(T_q) \tag{12}$$

or

$$f(T_q) = \frac{1}{T_q}. \tag{12a}$$

It should be noted that the interval T_q, for a large number of signals (e.g. a broad class of frequency - modulated signals), varies its value in time, therefore it cannot be treated as the classically conceived vibration period. Accordingly, the practice became to call this interval a quasi - period, whereas its inverse, i.e. $1/T_q = f_q(T_q)$ was called the quasi - instantaneous frequency.

3. Construction and working principle of the system (T, f—V)

It follows from the considerations presented in Section 1 that for signals occurring in reality there are considerable difficulties in the range of the registration and measurement of changes of the instantaneous frequency. This fact encouraged the authors to undertake investigations with the intention towards the conceptual and construction development of a special system permitting the measurement of the value of the quasi-instantaneous frequency at any time of the duration of the signal. The system designed and built is characterized by that the instantaneous value of its output voltage is directly proportional to the quasi - period (T_q) of a signal (when output I is used (see Fig. 1)) or the quasi - instantaneous frequency (f_q) of the signal (when output II is used). The working principle of the system whose schematic diagram is shown in Fig. 1, is as follows. The signal analysed (see Fig. 2a), whose amplitude variation can be contained in the limits between 10 mV to 5 V, which corresponds to dynamics of about 50 dB, is fed to the amplifier - amplitude limiter (1). At the time of the zero crossing of the input signal (i.e. the transition from the

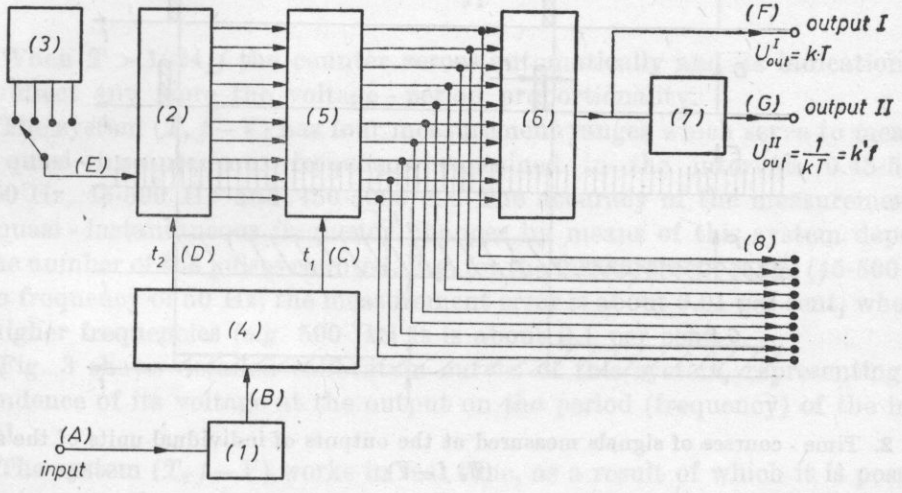

Fig. 1. A schematic diagram of the system (T, $f-V$)

1 — amplifier-amplitude limiter, 2 — binary counter, 3 — quartz generator, 4 — unit controlling the counter and memory, 5 — digital memory, 6 — digital-to-analog converter, 7 — analog divider, 8 — digital output

value "+" to "−"), the limiter gives a rising slope of a rectangular wave (see Fig. 2b). At that moment, the system which controls the counter and memory (4) generates a pulse with the duration $t_1 \cong 0.6$ μs (see Fig. 2c). This pulse causes the current state of the counter (2) to be "written" into the memory (5). Till the next zero crossing (counted with the same phase, i.e. from "+" to "−"), namely in the interval T, the pulse counter counts pulses with constant frequencies of 0.463, 4.63, 46.3 or 463 kHz (depending on the measurement range) generated by the quartz generator (3). The number of pulses counted is thus proportional to the period of the signal investigated, i.e. inversely proportional to its frequency. After the period T, the state of the counter (2) is put into the memory (5). Subsequently, by means of a digital - to - analog converter (6), the state of the counter (2) is transformed into a signal with constant voltage U_{out}, proportional to the number of the pulses memorized,

$$U_{out}^{(I)} = kn = kTf_1, \tag{13}$$

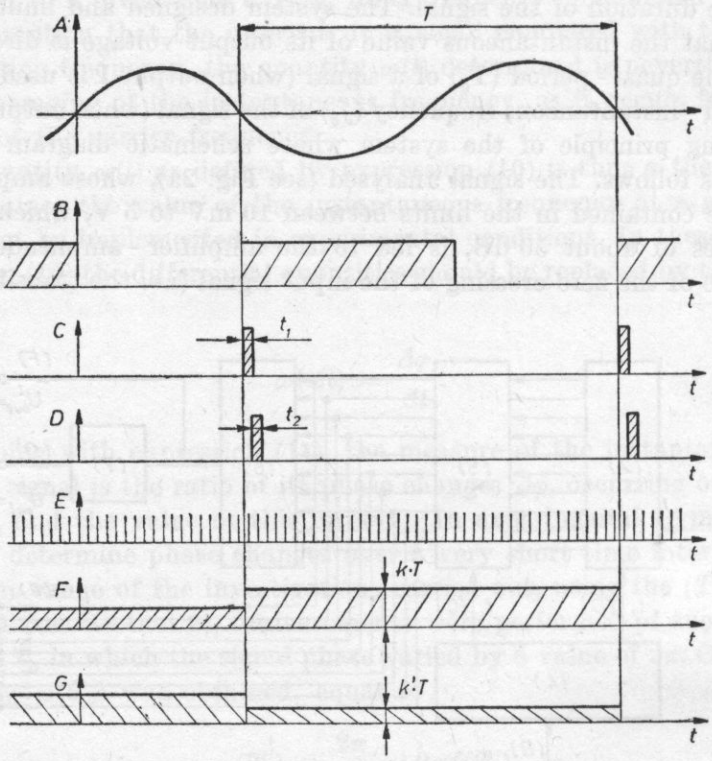

Fig. 2. Time - courses of signals measured at the outputs of individual units of the system (T, $f-V$)

A – time-course of a signal with a period T, B – signal with limited amplitude, C – pulse releasing the work of the counter and memory ($t_1 \simeq 0.6$ μs), D – pulse zeroing the counter ($t_2 \simeq 0.6$ μs), E – signal with the constant frequency f from a quartz generator, F – voltage time-course with a value proportional to the period of the input signal, G – voltage time-course with a value proportional to the frequency of the input signal

where $n = Tf_1$ is the number of the pulses memorized, T is the period of the input signal, f_1 is the frequency of the pulses from the quartz generator and k is the proportionality constant.

When output II is used, the value of the signal voltage $U_{out}^{(II)}$, as a result of using an analog divider (7), is

$$U_{out}^{(II)} = \frac{1}{kT} = k'f. \tag{13a}$$

Thus, this gives a relation of simple proportionality between the quasi-instantaneous frequency of the signal and the value of the output voltage of the system $(T, f-V)$.

After the pulses have been "written" into the memory (corresponding to the first period of the input signal) and transformed into a voltage signal, the control system (4) generates the pulse $t_2 \cong 0.6$ μs (see Fig. 2d), which causes the counter to be zeroed. Subsequently, the process of "counting" the pulses corresponding to the second period of the input signal is resumed, lasting until the moment of another zero crossing of this signal. Since the counter used in the system $(T, f-V)$ has a limited capacity ($2^{10} = 1024$), its correct performance requires that the following condition should be satisfied:

$$n = Tf_1 \leqslant 1024 \tag{14}$$

or otherwise,

$$T \leqslant \frac{1024}{f_1}. \tag{15}$$

When $T > 1024/f$ the counter zeroes automatically and its indications do not reflect any more the voltage - period proportionality.

The system $(T, f-V)$ has four measurement ranges which serve to measure the quasi - instantaneous frequency contained in the intervals 0.45-5 Hz, 4.5-50 Hz, 45-500 Hz and 450-5000 Hz. The accuracy of the measurement of the quasi - instantaneous frequency changes by means of this system depends on the number of the pulses counted. E.g. for the measurement range (45-500 Hz) and a frequency of 50 Hz, the measurement error is about 0.01 per cent, whereas for higher frequencies (e.g. 500 Hz) it is about 0.1 per cent.

Fig. 3 shows detailed calibration curves of this system, representing the dependence of its voltage at the output on the period (frequency) of the input signal.

The system $(T, f-V)$ works in real time, as a result of which it is possible to register continuously the changes of the quasi - instantaneous frequency of the signal investigated by means of an oscilloscope, for instance. Using the relation $U_{out}^{(II)}[V] \sim f[\text{Hz}]$, it is possible, after adequate calibration of the axis

Y of the oscilloscope, to read out directly the value of the quasi-instantaneous frequency of the signal in time. Figs. 5 and 6 show as an example a few oscillograms representing the time - course (lower curve) and the corresponding changes in the quasi - instantaneous frequency (upper curve) for some chosen signals. The oscillogram - based method for the determination of the quasi - instantaneous frequency is rather time consuming in practice, and also the read out itself involves some error. Much more accurate results are obtained

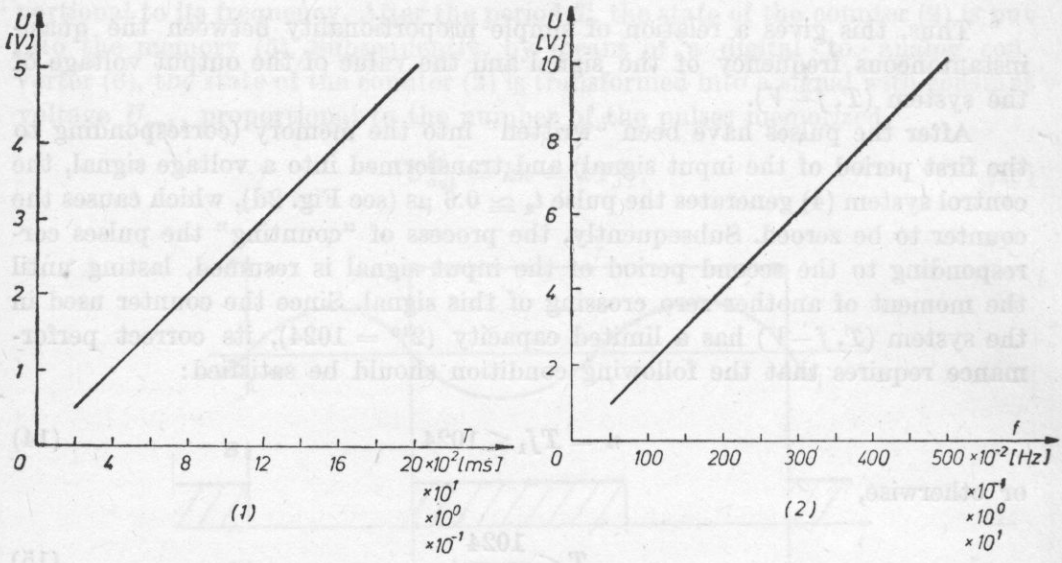

Fig. 3. Dependence of voltage on the period of the signal measured at the measurement output I (1) and the dependence of voltage on the frequency of the signal measured at the measurement output II (2) (for four measurement ranges)

using the digital method of signal processing. The principle of this method is the change of the voltage behaviour obtained at the output of the system (T, $f-V$) into discrete values, in a process of signal digitization. The series of numerical values obtained by this process constitutes input data for the computer with which the measurement results are elaborated.

Over the range of investigation, the process of the change of the analog signal obtained at the output of the system ($T, f-V$) into a digital one was carried out by means of a BK 7502 type digital event recorder.

Fig. 4 shows a schematic diagram of the full apparatus set-up by means of which it is possible to register changes in the quasi - instantaneous frequency of any signals, in particular transient behaviour. This set - up was used, for instance, to determine changes in the quasi - instantaneous frequency of transient signals in a room [1].

The apparatus set - up shown in Fig. 4 has the following working principle. An acoustic signal detected by the microphone (1) is, after amplification by the amplifier (2), fed to the input of the system $(T, f-V)$ (3). At the same time, this signal is registered by an oscilloscope with a delay line (5), which plays the role of a system delaying the moment of the release of the work of the digital event recorder (4). The oscilloscope (5) has a delay line permitting smooth motion along the time axis of a special marker by means of which it is

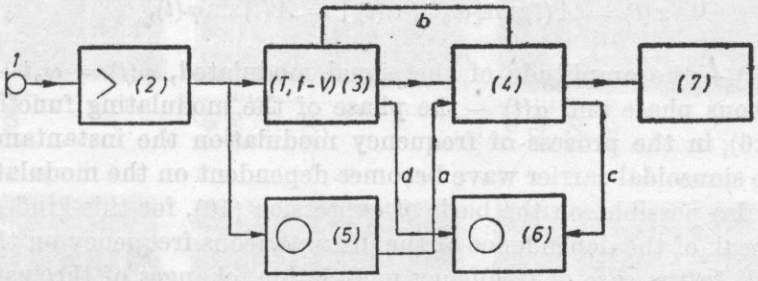

Fig. 4. A schematic diagram of the apparatus set - up for analog-digital registration of changes of the quasi - instantaneous frequency

1 – measurement microphone, *2* – microphone amplifier, *3* – system $(T, f-V)$, *4* – BK 7502 digital event recorder, *5* – oscilloscope with a delay line, *6* – control oscilloscope, *7* – Riad R20 computer, *a* – circuit releasing device 4 (Ext. Trigger), *b* – circuit controlling the sampling process, *c*, *d* – control circuits for signals at the outputs of devices *4* and *5*

possible to determine the beginning of the record of the time section of the signal of interest (e.g. the beginning of the process of sound decay in a room). At the moment when the signal registered reaches the position of the time marker on the oscilloscope display, the oscilloscope (5) generates a voltage pulse which, when fed to the digital event recorder (4), causes the release of its working cycle. From this moment on, the signal from the system $(T, f-V)$ is recorded in digital form in the memory of the device (4). The digital event recorder (4) is connected additionally to the system $(T, f-V)$ by the circuit (*b*) controlling the sampling process of the device (4). By using the oscilloscope (6), it is possible to control visually the work of the system $(T, f-V)$ (4) and to control the content of the memory of the digital event recorder (4). The data contained in the memory of the device (4) are then introduced into the operational system of a Riad R20 computer (7). From this moment on, these data can undergo any mathematical operations carried out by the computer, according to the computer programme introduced.

4. Measurement results

Fig. 5 shows as an example a few oscillograms obtained by the process of calibrating the system $(T, f-V)$ built. The lower curves in these oscillograms

illustrate the time - courses of test signals which were: amplitude - modulated (1), frequency - modulated (2) and simultaneously amplitude and frequency modulated (3), successively by linear (*a*), sinusoidal (*b*) and triangular (*c*) functions. In turn, the upper curves illustrate changes of the quasi - instantaneous frequency (f_q) corresponding to the signals obtained at the output (II) of the system ($T, f-V$). The frequency - modulated signal in Fig. 5 can be described in general by the expression

$$x(t) = A(t)\sin[\omega_0 t + a(t)] = A(t)\sin\varphi(t), \tag{16}$$

where $A(t)$ – the amplitude of the signal modulated, $\varphi(t) = \omega_0 t + a(t)$ – the instantaneous phase and $a(t)$ – the phase of the modulating function. According to (16), in the process of frequency modulation the instantaneous phase $\varphi(t)$ of the sinusoidal carrier wave becomes dependent on the modulating signal.

It is also possible, on the basis of expression (10), for this kind of modulation, to speak of the dependence of the instantaneous frequency on the modulating signal. In the case of frequency modulation, changes of the instantaneous frequency of the modulated signal are proportional to the modulating one, i.e.

$$\omega(t) = \omega_0 + a\beta(t). \tag{17}$$

In turn the instantaneous phase of the modulated signal changes in proportion with the intergal of the modulating signal

$$\varphi(t) = \omega_0 t + a\int \beta(t)\,dt. \tag{18}$$

The functions $\beta(t)$, successively in linear, sinusoidal and triangular forms, correspond to the modulated signals shown in Fig. 5.2a, b, c.

As was mentioned above over the range of the investigations performed measurements were carried out over such a time interval $\Delta t = T_q$ in which the phase of the signal varied by a value of 2π. As a result of this, no exact values of the instantaneous frequency, according to (10a), but some approximation of it, which was called quasi - instantaneous frequency, was obtained (see 12a). Changes of this frequency in time, recorded at output II of the system ($T, f-V$) for the modulated signals mentioned above, are illustrated by Fig. 5.2a, b, c. It is seen in this figure that changes of the quasi - instantaneous frequency reflect faithfully the modulating functions prescribed in the test signals; i.e. linear, sinusoidal and triangular ones. In addition, on the basis of comparison of the records given in lines *a*, *b* and *c* in Fig. 5, essential conclusions can be drawn about the accuracy of the indications of the system ($T, f-V$) in the case of signals whose amplitude varies in time. For this purpose, Fig. 5.1a, b, c shows the time - courses of a sinusoidal signal modulated only in terms of amplitude by means of linear, sinusoidal and triangular functions.

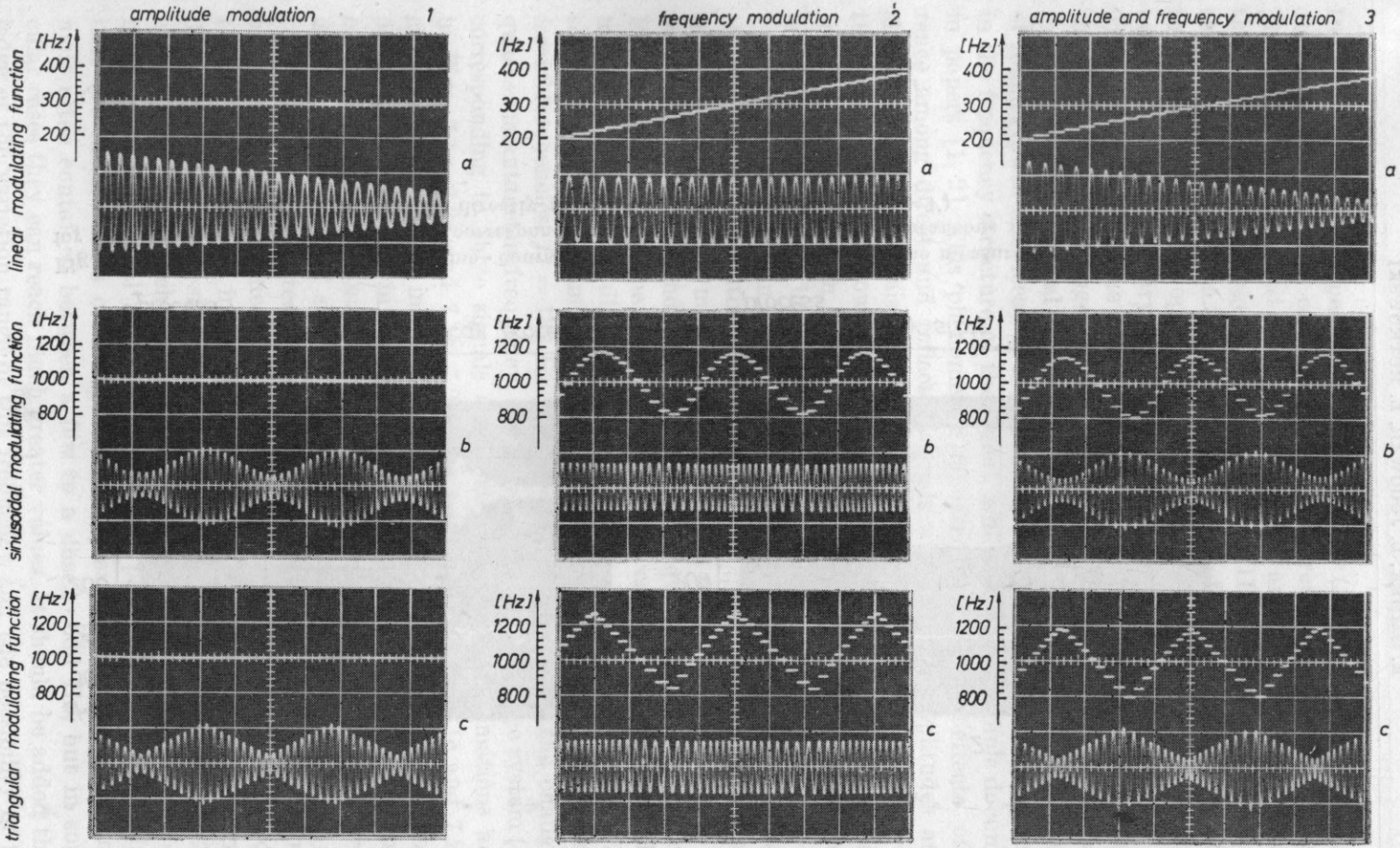

Fig. 5. Oscillograms of the time - course of test signals: amplitude - modulated (1), frequency - modulated (2), amplitude and frequency modula ted(3), for modulating functions: linear (a), sinusoidal (b) and triangular (c) (lower curves), and thec erresponding records of the quasi - instantaneous frequency (upper curves), registered directly at output II of the system (T, $f-V$)

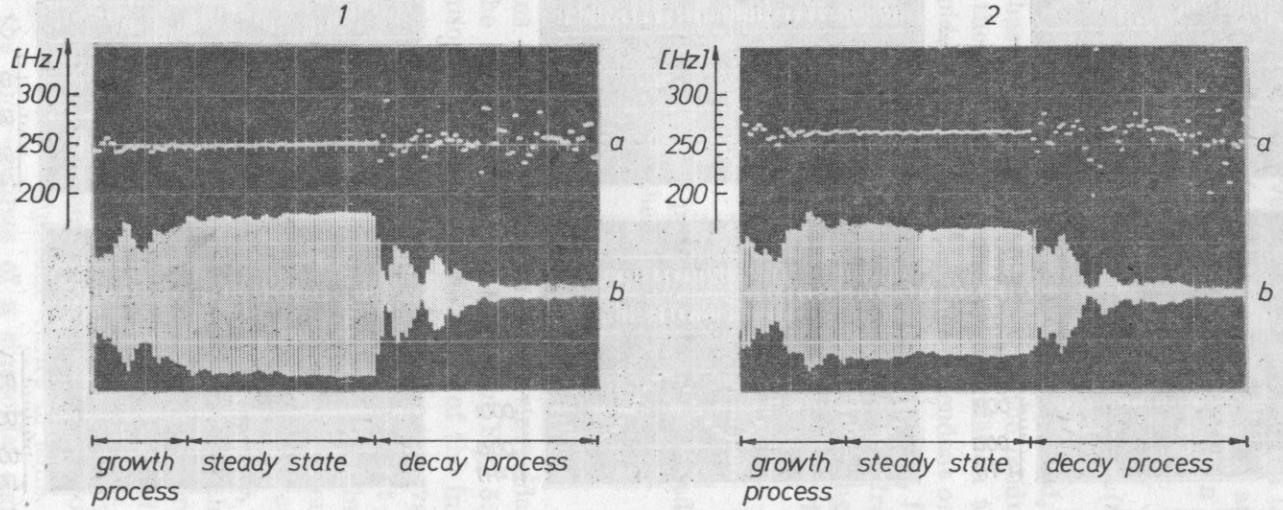

Fig. 6. Oscillograms of the signal time - course (1*b* and 2*b*) obtained at the same measurement point in a room for two different frequencies and the corresponding changes of the quasi - instantaneous frequency (1*a* and 2*a*) registered directly at output II of the system (T, $f-V$)

In such a case, at output II of the system $(T, f-V)$ constant voltage is obtained whose value corresponds to the frequency of the filling signal. The signals which are at the same amplitude and frequency modulated and the corresponding voltage changes at output II of the system $(T, f-V)$ are shown in turn in Fig. 5.3a, b, c. Comparison of Figs. 5.1 and 5.3 shows that the system $(T, f-V)$ operates well also for signals with not only frequency but also amplitude varying in time, which are most frequent in practice. These facts confirm the full usefulness of this system in investigations of the more complex changes in this frequency with fluctuating nature, occurring in a number of physical phenomena. One of these phenomena is the process of sound growth and decay in a room in which it is possible to observe changes in the frequency structure of the signal, which was given ample documentation in papers [1, 2]. This phenomenon is based on complex effects of interference among direct and reflected signals with various amplitudes and phase shifts. As a result of this, the resultant time - course of the sound pressure in the process of sound growth and decay can be regarded as one whose amplitude and phase vary in time, which, as was mentioned above, is related to a definite change in the instantaneous frequency.

Fig. 6 shows as an example two oscillograms of the signal time - course (1b and 2b) with a distinctly seen process of growth, steady state and decay, registered at the same measurement point in a room for two different frequencies and the corresponding changes in the quasi - instantaneous frequency. Fig. 7 shows in turn the results obtained in a concert hall by using the equipment whose schematic diagram is shown in Fig. 4. The oscillograms (7.1b, 7.2b) seen in Fig. 7 correspond to the time - course of signals registered for two different frequencies, $f_1 = 139$ Hz and $f_2 = 141$ Hz. In turn, the changes of the quasi - instantaneous frequency, registered at output II of the system $(T, f-V)$, corresponding to these signals and their quantitative estimations are shown in Figs. 7.1*a*, 7.2*a* and 7.1*c*, 7.2*c*. The solid line in Fig. 7.1*c* and 7.2*c* denote changes of the quasi - instantaneous frequency of the signal as averaged over 50 ms time intervals; in turn, the vertical lines represent the extreme values of these changes. The numbers given on the left (i.e. $f = 139$ Hz, $f = 141$ Hz) are the frequencies of signals transmitted into the room.

The results presented in Fig. 7 show that the range and character of changes of the quasi - instantaneous frequency depend essentially on the frequency of the signal transmitted into the room and the time interval of the signal considered. A detailed analysis of the investigations of this phenomenon [1, 2] showed a large complexity of changes in the quasi - instantaneous frequency, occurring in the transient signal in the room. It was possible to determine in general that the mean values of changes of the quasi - instantaneous frequency are most often contained between a few to a dozen - odd Hz, but in some particular cases they can reach much greater values. It should be added that knowledge of the variation range of this frequency and the possibility of their per-

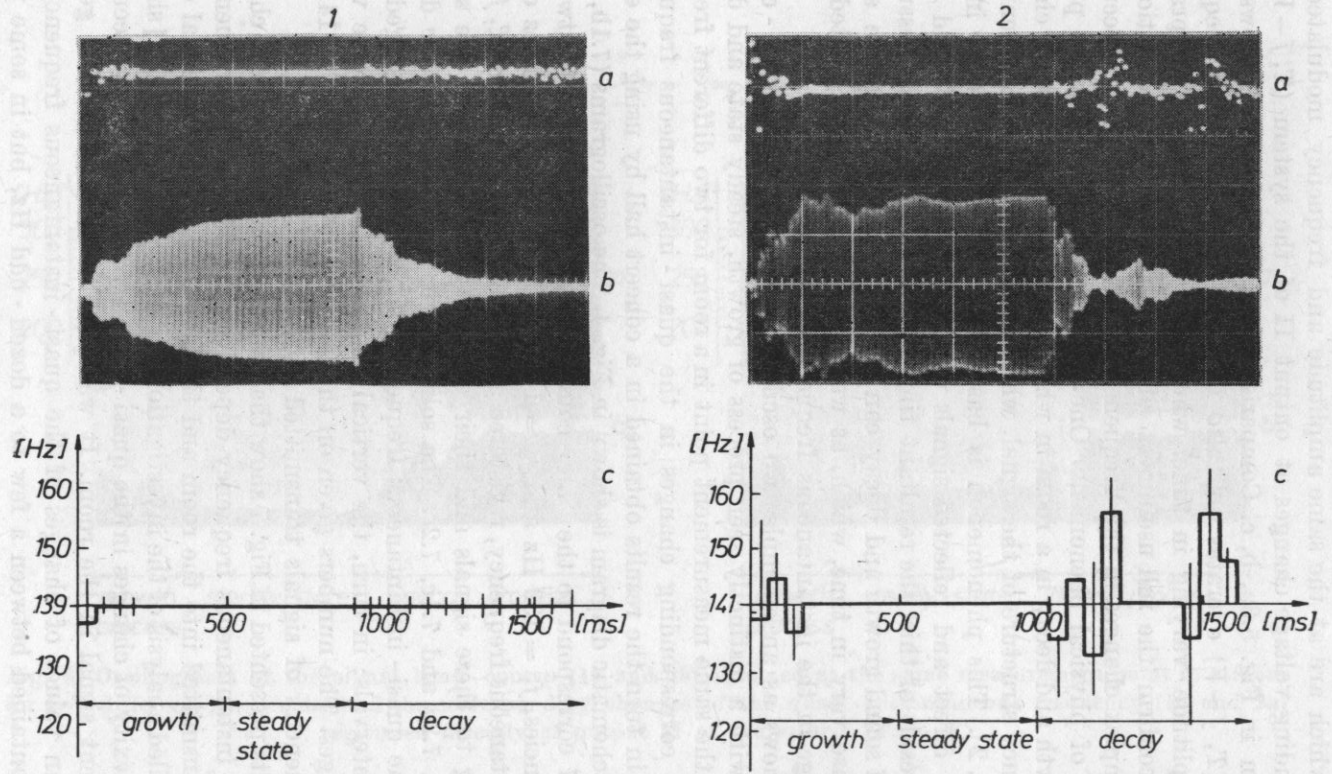

Fig. 7. Oscillograms of the signal courses (1*b* and 2*b*) registered in a concert hall for two different frequencies and the corresponding changes of the quasi-instantaneous frequency registered directly at output II of the system $(T, f-V)$ (1*a* and 2*a*) and at the output of unit 7 (see Fig. 4) (1*c* and 2*c*)

ception by listeners can have in practice an essential effect on the resultant, subjective evaluation of the acoustic properties of rooms.

In conclusion, it is interesting to note that instantaneous changes (fluctuations) of frequency nearly always accompany in practice sounds of speech, music and a large number of other acoustic phenomena and processes. Thus, better knowledge of these changes and their quantitative estimation can be important elements of the investigations of the time and spectral structure of these processes and phenomena.

The authors wish to express their gratitude to Mr. A. SKUMIEL, M. Sc., for his valuable contribution to the construction of the system $(T, f-V)$, which was patented.

The research was carried out within the Problem MR. I. 24.

References

[1] E. OZIMEK, J. L. JUGOWAR, L. RUTKOWSKI, *Determination of changes of the instantaneous frequency of the transient signals propagating in a room, depending on its chosen acoustic parameters* (in Polish), Report MR. 1. 24. XIII. 7, Poznań 1982 (*prepared for publication*).

[2] J. L. JUGOWAR, *Analysis of frequency changes of transient state of sound propagating in a room*, Lectures of 8th Colloquium on Acoustics, Budapest 1982.

[3] S. O. RICE, *Mathematical analysis of random noise*, Bell System Tech. J., **23**, 24 (1944/45).

Received on 8 March, 1984.

C H R O N I C L E

REVIEW

V. Ilgunas, E. Jaronis, V. Sukackas, *Ultrasonic interferometry* (in Russian), Vilna 1983

The monograph gives the theoretical fundamentals and the results of experimental research carried out in the ultrasonic laboratory of the Polytechnical Institute in Kaunas, headed by Prof. Barsauskas. In addition to a complex representation of the problems of ultrasonic interferometry, the book contains a number of original achievements of its authors, which deserve above all attention.

The authors were the first to draw attention to systematic measurement error caused by the diffraction effect in interferometers. This led to the introduction of correlation of the sound velocity measurements, assumed universally as standard ones, in distilled water, carried out by the US Bureau of Standards.

The method developed by the authors permits the measurement of the absorption coefficient of liquids with weak absorption, which had previously been very difficult. The authors also give original designs of interferometer for the investigation of liquids with strong absorption and a two - chamber interferometer for measurements of liquids with weak concentration. They developed an interferometer with an open focussing resonator, permitting measurements ower the low ultrasonic range, from 20 kHz on. The noveltres are also interferometric methods for direct measurements of acoustic impedance and liquid density. The authors also describe high - class interferometers used in their laboratory for the purposes of metrology and scientific research. In the theoretical part, the authors analyse the mathematical model of an interferometer, taking into account the phenomena of diffraction and the formation of waveguides. They consider piezoelectric transducers from the point of view of their performance in interferometers.

The book contains a multi - sided analysis of the error involved in interferometric measurements and the shortcomings and advantages of the different interferometer types. The book is a valuable piece of ultrasonic literature, useful in particular for researchers in centres engaged in molecular acoustics

Ignacy Malecki
(Warsaw)